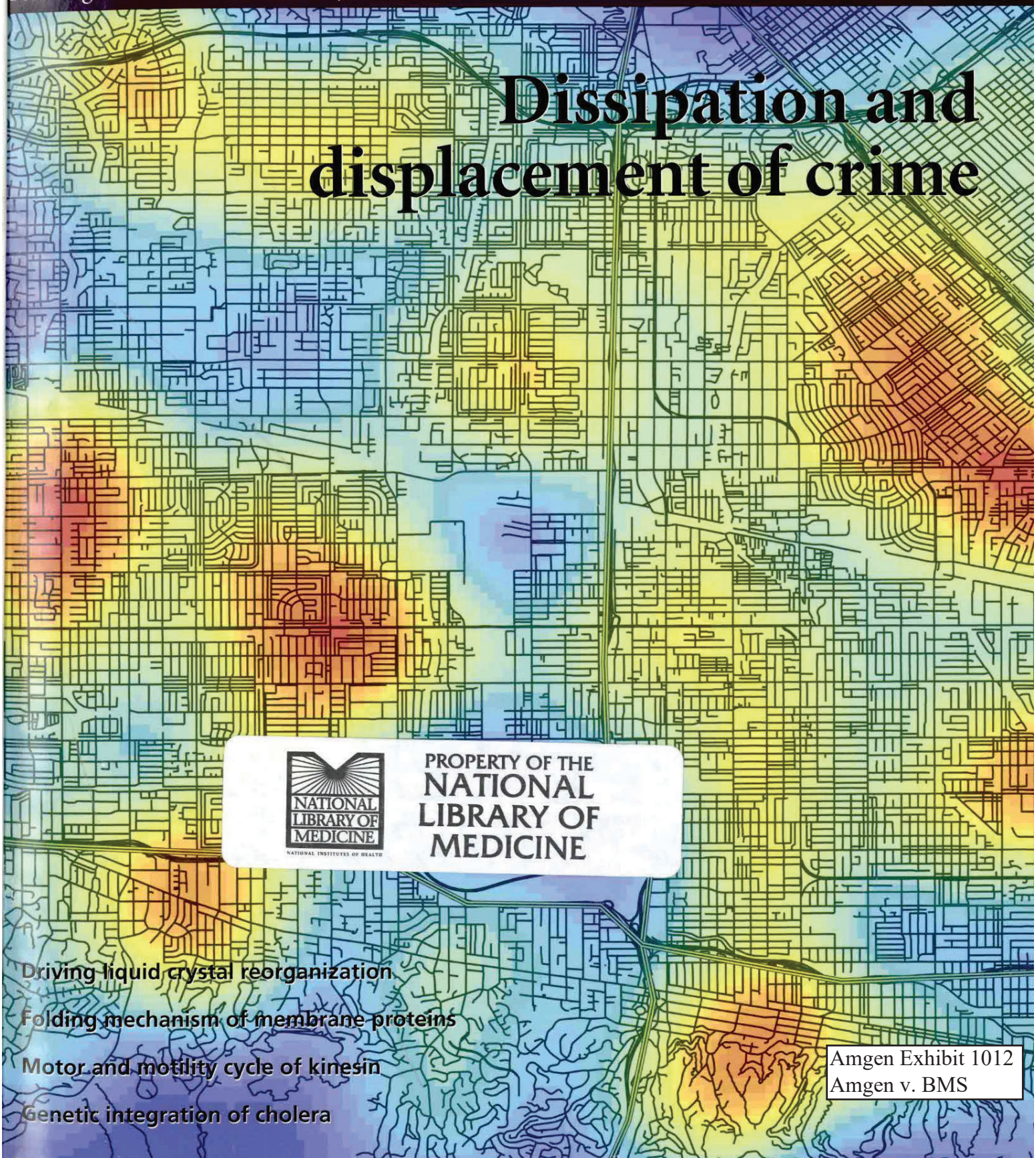
rch 2, 2010 | vol. 107 | no. 9 | pp. 3943–4486

Proceedings of the National Academy of Sciences
v. 107, no. 9 (Mar. 2 2010)
General Collection
W1 PR586A
2010-03-23 10:43:41

PNAS

oceedings of the National Academy of Sciences of the United States of America www.pnas.org



Dissipation and displacement of crime

PROPERTY OF THE
NATIONAL
LIBRARY OF
MEDICINE

Driving liquid crystal reorganization

Folding mechanism of membrane proteins

Motor and motility cycle of kinesin

Genetic integration of cholera

Amgen Exhibit 1012
Amgen v. BMS

NATIONAL LIBRARY OF MEDICINE
NLM 04605417 8

DFA374 PA 197
05-26-11 13270 XL



National Academy of Sciences
500 Fifth Street, NW
Washington, DC 20001

PNAS
Proceedings of the National Academy of Sciences of the United States of America www.pnas.org

PRESIDENT OF THE ACADEMY
Ralph J. Cicerone

EDITOR-IN-CHIEF
Randy Schekman

ASSOCIATE EDITORS
David Chandler
Alan Fersht
Jack Halpern
Dolores R. Piperno
Solomon H. Snyder
B. L. Turner II
Peter K. Vogt
Susan R. Wessler

EDITORIAL BOARD

Animal, Nutritional, and Applied Microbial Sciences
David L. Denlinger
R. Michael Roberts
Linda J. Saif
Ryuzo Yanagimachi

Anthropology
Richard G. Klein
James F. O'Connell
Alan Walker

Applied Mathematical Sciences
Peter J. Bickel
David L. Donoho

Applied Physical Sciences
Noel A. Clark
Francisco de la Cruz
Harry L. Swinney

Astronomy
Neta A. Bahcall

Biochemistry
Michael R. Botchan
Jennifer A. Doudna
Edward D. Korn
Stephen C. Kowalczykowski
John Kuriyan
Michael A. Marletta
Kiyoshi Mizuuchi
Charles M. Radding
Venkatraman Ramakrishnan
Tom A. Rapoport
James A. Wells
William T. Wickner

Biophysics and Computational Biology
David Baker
Adriaan Bax
William A. Eaton
Angela M. Gronenborn
Barry H. Honig
Robert Langer
Michael Levitt
Gregory A. Petsko

Cellular and Developmental Biology
C. David Allis
Donald D. Brown
Eric H. Davidson
Brigid L. M. Hogan
Eric N. Olson
Michael Rosbash
David D. Sabatini
Gertrud M. Schüpbach

Cellular and Molecular Neuroscience
Pietro V. De Camilli
Richard L. Huganir
L. L. Iversen
Yuh Nung Jan
Eve Marder
Jeremy Nathans
Charles F. Stevens
Thomas C. Südhof
Joseph S. Takahashi
Richard W. Tsien

Chemistry
Stephen J. Benkovic
Harry B. Gray
Michael L. Klein
Raphael D. Levine
Jerrold Meinwald
Nicholas J. Turro

Computer and Information Sciences
William H. Press

Economic Sciences
Roy Radner
Jose A. Scheinkman

Engineering Sciences
Evelyn L. Hu
Katepalli R. Sreenivasan

Environmental Sciences and Ecology
Robert E. Dickinson
David M. Karl
Robert May
David W. Schindler

Evolutionary Biology
Francisco J. Ayala
May R. Berenbaum
Sean B. Carroll
W. Ford Doolittle
Douglas J. Futuyma
Daniel L. Hartl
Masatoshi Nei
Gene E. Robinson

Genetics
Kathryn V. Anderson
Thomas W. Cline
Stanley N. Cohen
Barry Ganetzky
Iva S. Greenwald
Jeffrey C. Hall
Philip C. Hanawalt
Rudolf Jaenisch
Mary-Claire King
Jasper Rine
Reed B. Wickner

Geology
W. G. Ernst
James P. Kennett

Geophysics
Mark H. Thiemens

Human Environmental Sciences
Ruth S. DeFries
Susan Hanson

Immunology
Peter Cresswell
Douglas T. Fearon
Tak Wah Mak
Philippa Marrack
William E. Paul
Ralph M. Steinman
Tadatsugu Taniguchi
Arthur Weiss

Mathematics
Richard V. Kadison
Robion C. Kirby

Medical Genetics, Hematology, and Oncology
C. Thomas Caskey
Joseph L. Goldstein
Mark T. Groudine
Tony Hunter
Philip W. Majerus
Inder M. Verma

Medical Physiology and Metabolism
Charles A. Dinarello
Robert J. Lefkowitz
Salvador Moncada
David W. Russell

Microbial Biology
John M. Coffin
R. John Collier
Emil C. Gotschlich
E. Peter Greenberg
Diane E. Griffin
Peter M. Howley
Ralph R. Isberg
Elliott D. Kieff
Robert A. Lamb
Peter Palese
Thomas E. Shenk
Thomas J. Silhavy
Thomas E. Wellems

Physics
Anthony Leggett
Paul C. Martin
José N. Onuchic

Physiology and Pharmacology
Richard W. Aldrich
Susan G. Amara
David Julius
Arthur Karlin
Ramón Latorre

Plant Biology
David Baulcombe
Anthony R. Cashmore
Maarten J. Chrispeels
Enrico Coen
Joseph R. Ecker
Robert Haselkorn
June B. Nasrallah

Plant, Soil, and Microbial Sciences
Roger N. Beachy
James C. Carrington
Brian J. Staskawicz

Psychological and Cognitive Sciences
Dale Purves
Edward E. Smith

Social and Political Sciences
Alejandro Portes
Brian Skyrms
Kenneth W. Wachter

Sustainability Science
Barry R. Bloom
William C. Clark
Partha Sarathi Dasgupta
Robert W. Kates
Pamela A. Matson
Hans Joachim Schellnhuber

Systems Biology
Marc W. Kirschner

Systems Neuroscience
Thomas D. Albright
Robert Desimone
Fred H. Gage
Charles D. Gilbert
Marcus E. Raichle
Leslie G. Ungerleider

Submission to PNAS
Authors (members and nonmembers) may submit their manuscripts directly to PNAS at www.pnascentral.org. Authors must recommend three appropriate Editorial Board members, three NAS members who are expert in the paper's scientific area, and five qualified referees. No Academy member sponsor is required.

PNAS

Proceedings of the National Academy of Sciences of the United States of America www.pnas.org

PNAS (ISSN-0027-8424) is published weekly in print by the National Academy of Sciences.

Correspondence: PNAS, 700 11th Street, NW, Suite 450, Washington, DC 20001 USA. E-mail: PNAS@nas.edu.

Copyright: Volumes 90–105, copyright © 1993–2008 by the National Academy of Sciences of the United States of America, all rights reserved. Volumes 1–89 and 106–107, copyright as a collective work only; author(s) retains copyright to individual articles. **Requests for Permission:** See www.pnas.org/misc/rightperm.shtml for details. Address requests to reproduce material published in Volumes 1–89 to the original author(s); e-mail other requests to PNASpermissions@nas.edu, fax 1-202-334-2739, or PNAS Permissions Editor, 700 11th Street, NW, Suite 450, Washington, DC 20001 USA. Please cite the exact material to be reprinted and state specifically where it will be used. **Photocopies:** PNAS is registered with the Copyright Clearance Center (CCC), 222 Rosewood Drive, Danvers, MA 01923 USA, fax 1-978-750-4470, or www.copyright.com. Authorization to photocopy items for the internal or personal use of specific clients is granted by the National Academy of Sciences provided that the proper fee is paid directly to CCC. **Microforms:** Contact UMI at www.umi.com or P.O. Box 1346, Ann Arbor, MI 48106-1346 USA.

Advertising: Mark Chesnek, 700 11th Street, NW, Suite 450, Washington, DC 20001 USA. Phone 1-202-334-2696, fax 1-202-334-1346, e-mail mchesnek@nas.edu.

Subscriptions: Send payments to PNAS, c/o AIP, P.O. Box 503284, St. Louis, MO 63150-3284 USA. For subscription help, e-mail subs@aip.org, phone 1-516-576-2270, or visit www.pnas.org/subscriptions. **2010 Rates:** US, individual–$375 (first class delivery available at a surcharge of $315); non-US, individual–$585; US/non-US, institutional online only, $1,305–7,215. Subscriptions are entered on a calendar-year basis. **Exclusive Agent for Subscribers in Japan:** USACO Corporation, 17-12 Higashi-Azabu, 2-Chome, Minato-ku, Tokyo 106-0044, Japan. Phone 81 3 3505 3256, fax 81 3 3505 6282, e-mail tokyo-sales@usaco.co.jp. **Change of Address:** PNAS, c/o AIP, Suite 1NO1, 2 Huntington Quadrangle, Melville, NY 11747 USA. Phone 1-800-344-6902, fax 1-516-349-9704, e-mail subs@aip.org. Please send notification 6 weeks in advance and list the old and new addresses. **Claims:** Requests for replacement copies will not be honored more than 60 days after the issue date for domestic subscribers and not more than 90 days after the issue date for foreign subscribers. Claims will not be honored for more than two issues per calendar year for the same subscriber. To make a claim, e-mail subs@aip.org or call 1-800-344-6902. **Single Copies:** $40 per issue in the US, $50 non-US To order, e-mail subs@aip.org or call 1-800-344-6902. **Canadian GST:** Registration Number R-133130880.

Postmaster: Send address changes to PNAS, c/o AIP, Suite 1NO1, 2 Huntington Quadrangle, Melville, NY 11747 USA. Periodicals postage paid at Washington, DC, and additional mailing offices.

PNAS is available online at www.pnas.org.
PRINTED IN THE USA

Printed on acid-free paper effective Volume 84, Issue 1, and on 80% post-consumer recycled paper effective Volume 107, Issue 1. Printed with soy ink.

PNAS STAFF

Publisher
Kenneth R. Fulton

Executive Editor
Diane M. Sullenberger

Managing Editor
Daniel H. Salsbury

Recruiting Editor
David Stopak

Editorial Staff
James B. Allison
Josiah W. Armour
Kirti Chadha
Tom J. Colihan
Ryan Conley
Matt Demarest
Julia M. Diez d'Aux
Kathleen E. Dugan
Meredith C. Jones
Nicole Joy
Etta Kavanagh
Jacob Kendall-Taylor
Sarah Leamy
Kay McLaughlin
Megan Miller
Kathryn Murphy
Tom Myers
Prashant Nair
Jennifer Nelson
N. T. Ngo
May B. Piotrowski
Allison Ross
Amy Whitcomb

Production Manager
Dana M. Compton

Production Staff
Barbara A. Bacon
Sophie Mohin
Kelly A. Newton
Kat Rodenhizer
Audrey Springer

Marketing Manager
Mark Chesnek

Marketing Staff
Jennifer Bradley

Media Staff
Sola Ayeni-Biu
Todd Johnston
Jonathan Lifland
Jenny Ruth Morber
Ashley Truxon

Finance Manager
Simone Marshall-Campbell

Business Staff
Metina Booze
Juanita Culler
Sara Spizzirri

Authorship
Authorship should be limited to those who have contributed substantially to the work. Authors must indicate their specific contributions to the published work; this information will be published as a footnote to the paper. The corresponding author must have obtained permission from all authors for the submission of each version of the paper and for any change in authorship.

Conflict of Interest
All authors, members, referees, and editors must disclose any association that poses a conflict of interest in connection with the manuscript. Authors must acknowledge all funding sources supporting the work. See www.pnas.org/misc/coi.shtml for details.

Supporting Information
Authors may use Supporting Information to enhance their papers in PNAS by providing additional substantive material for online posting, but the print version of the paper must stand on its own merits.

Cover Images
Authors are encouraged to submit scientifically interesting and visually arresting images for the cover.

Information for Authors
Please see the complete Information for Authors, available online at www.pnas.org.

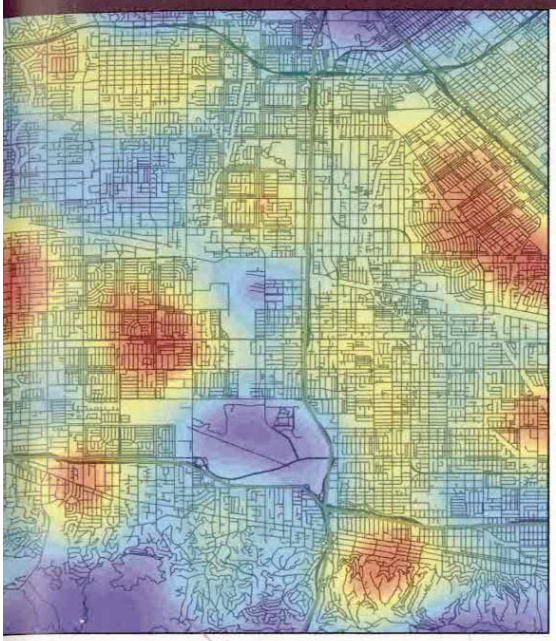
PNAS Online
PNAS articles are published daily online before print at www.pnas.org in PNAS Early Edition.

The articles in PNAS report original research by independent authors and do not necessarily represent the views of the National Academies.

March 2, 2010 | vol. 107 | no. 9 | 3943–4486

PNAS

Proceedings of the National Academy of Sciences of the United States of America www.pnas.org



Cover image: Pictured are residential burglary hotspots in a portion of Los Angeles, California. Martin B. Short et al. report on reaction-diffusion models indicating that spatial crime patterns come in two fundamental types: supercritical hotspots, which emerge from small stochastic fluctuations in crime, and subcritical hotspots, which emerge from large spikes in crime. The authors suggest that policing tactics focused on supercritical hotspots can displace the hotspot into a ring structure, which then breaks up into new hotspots, whereas tactics focused on subcritical hotspots may result in lasting crime dissipation. See the article by Short et al. on pages 3961–3965. Image courtesy of P. Jeffrey Brantingham.

From the Cover

3961 Dissipation and displacement of crime

3998 Driving liquid crystal reorganization

4099 Folding mechanism of membrane proteins

4111 Motor and motility cycle of kinesin

4377 Genetic integration of cholera

Contents

THIS WEEK IN PNAS

3943 **In This Issue**

LETTERS (ONLINE ONLY)

E29 **Distant friends, close strangers? Inferring friendships from behavior**
jimi adams

E31 **Reply to adams: Multi-dimensional edge inference**
Nathan Eagle, Aaron Clauset, Alex (Sandy) Pentland, and David Lazer

COMMENTARIES

3945 **Liquid crystals enable chemoresponsive reconfigurable colloidal self-assembly**
Ivan I. Smalyukh
→ *See companion article on page 3998*

3947 **Membrane protein folding makes the transition**
Paula J. Booth and Jane Clarke
→ *See companion article on page 4099*

3949 **Kinesin motor activation: Microtubules pull the switches**
Franck Fourniol and Carolyn A. Moores
→ *See companion article on page 4111*

3951 **Efficiency and specificity of CTXϕ chromosomal integration: *dif* makes all the difference**
E. Fidelma Boyd
→ *See companion article on page 4377*

INAUGURAL ARTICLE

3953 **Vaccination with partial knowledge of external effectiveness**
Charles F. Manski

PHYSICAL SCIENCES

APPLIED MATHEMATICS

3961 **Dissipation and displacement of hotspots in reaction-diffusion models of crime**
Martin B. Short, P. Jeffrey Brantingham, Andrea L. Bertozzi, and George E. Tita

APPLIED PHYSICAL SCIENCES

3966 **Systemic antiangiogenic activity of cationic poly-L-lysine dendrimer delays tumor growth**
Khuloud T. Al-Jamal, Wafa' T. Al-Jamal, Simon Akerman, Jennifer E. Podesta, Açelya Yilmazer, John A. Turton, Alberto Bianco, Neil Vargesson, Chryso Kanthou, Alexander T. Florence, Gillian M. Tozer, and Kostas Kostarelos

Free online through the PNAS open access option.

3972 **Field-effect-tuned lateral organic diodes**
Bal Mukund Dhar, Geetha S. Kini, Guoqiang Xia, Byung Jun Jung, Nina Markovic, and Howard E. Katz

3977 **Learning as a phenomenon occurring in a critical state**
Lucilla de Arcangelis and Hans J. Herrmann

CHEMISTRY

3982 **Insight into the mechanism of an iron dioxygenase by resolution of steps following the Fe^{IV}=O species**
Piotr K. Grzyska, Evan H. Appelman, Robert P. Hausinger, and Denis A. Proshlyakov

3988 **Targeted metabolic labeling of yeast N-glycans with unnatural sugars**
Mark A. Breidenbach, Jennifer E. G. Gallagher, David S. King, Brian P. Smart, Peng Wu, and Carolyn R. Bertozzi

3994 **A model for the CO-inhibited form of [NiFe] hydrogenase: synthesis of $(CO)_3Fe(\mu\text{-}S^tBu)_3Ni\{SC_6H_3\text{-}2,6\text{-}(mesityl)_2\}$ and reversible CO addition at the Ni site**
Yasuhiro Ohki, Kazunari Yasumura, Masaru Ando, Satoko Shimokata, and Kazuyuki Tatsumi

4299 **Disruption of angiogenesis and tumor growth with an orally active drug that stabilizes the inactive state of PDGFRβ/B-RAF**
Eric A. Murphy, David J. Shields, Konstantin Stoletov, Elena Dneprovskaia, Michele McElroy, Joshua I. Greenberg, Jeff Lindquist, Lisette M. Acevedo, Sudarshan Anand, Bharat Kumar Majeti, Igor Tsigelny, Adrian Saldanha, Breda Walsh, Robert M. Hoffman, Michael Bouvet, Richard L. Klemke, Peter K. Vogt, Lee Arnold, Wolfgang Wrasidlo, and David A. Cheresh

4341 **Only two amino acids are essential for cytolytic toxin recognition of cholesterol at the membrane surface**
Allison J. Farrand, Stephanie LaChapelle, Eileen M. Hotze, Arthur E. Johnson, and Rodney K. Tweten

COMPUTER SCIENCES

4069 **Markov random fields reveal an N-terminal double beta-propeller motif as part of a bacterial hybrid two-component sensor system**
Matt Menke, Bonnie Berger, and Lenore Cowen

ENGINEERING

3998 **Chemoresponsive assemblies of microparticles at liquid crystalline interfaces**
Gary M. Koenig, Jr., I-Hsin Lin, and Nicholas L. Abbott
→ *See Commentary on page 3945*

4004 **Ultrahigh-throughput screening in drop-based microfluidics for directed evolution**
Jeremy J. Agresti, Eugene Antipov, Adam R. Abate, Keunho Ahn, Amy C. Rowat, Jean-Christophe Baret, Manuel Marquez, Alexander M. Klibanov, Andrew D. Griffiths, and David A. Weitz

GEOLOGY

4010 **The Murray Springs Clovis site, Pleistocene extinction, and the question of extraterrestrial impact**
C. Vance Haynes, Jr., J. Boerner, K. Domanik, D. Lauretta, J. Ballenger, and J. Goreva

PHYSICS

4016 **Abduction and asylum in the lives of transcription factors**
Anat Burger, Aleksandra M. Walczak, and Peter G. Wolynes

4141 **Membrane curvature controls dynamin polymerization**
Aurélien Roux, Gerbrand Koster, Martin Lenz, Benoît Sorre, Jean-Baptiste Manneville, Pierre Nassoy, and Patricia Bassereau

SOCIAL SCIENCES

ECONOMIC SCIENCES

3953 **Vaccination with partial knowledge of external effectiveness**
Charles F. Manski

SOCIAL SCIENCES

3961 **Dissipation and displacement of hotspots in reaction-diffusion models of crime**
Martin B. Short, P. Jeffrey Brantingham, Andrea L. Bertozzi, and George E. Tita

BIOLOGICAL SCIENCES

BIOCHEMISTRY

4022 **A role for a bacterial ortholog of the Ro autoantigen in starvation-induced rRNA degradation**
Elisabeth J. Wurtmann and Sandra L. Wolin

4028 **Severe oxidative stress induces protein mistranslation through impairment of an aminoacyl-tRNA synthetase editing site**
Jiqiang Ling and Dieter Söll

4034 **Structural basis for the cooperative interplay between the two causative gene products of combined factor V and factor VIII deficiency**
Miho Nishio, Yukiko Kamiya, Tsunehiro Mizushima, Soichi Wakatsuki, Hiroaki Sasakawa, Kazuo Yamamoto, Susumu Uchiyama, Masanori Noda, Adam R. McKay, Kiichi Fukui, Hans-Peter Hauri, and Koichi Kato

4040 **The structure of the harmonin/sans complex reveals an unexpected interaction mode of the two Usher syndrome proteins**
Jing Yan, Lifeng Pan, Xiuye Chen, Lin Wu, and Mingjie Zhang

4046 **Pathway of ATP utilization and duplex rRNA unwinding by the DEAD-box helicase, DbpA**
Arnon Henn, Wenxiang Cao, Nicholas Licciardello, Sara E. Heitkamp, David D. Hackney, and Enrique M. De La Cruz

4051 **Stem cell-specific activation of an ancestral *myc* protooncogene with conserved basic functions in the early metazoan *Hydra***
Markus Hartl, Anna-Maria Mitterstiller, Taras Valovka, Kathrin Breuker, Bert Hobmayer, and Klaus Bister

4057 **Yeast Tdp1 regulates the fidelity of nonhomologous end joining**
Karim Bahmed, Karin C. Nitiss, and John L. Nitiss

4063 **Cell-specific differences in the requirements for translation quality control**
Noah M. Reynolds, Jiqiang Ling, Hervé Roy, Rajat Banerjee, Sarah E. Repasky, Patrice Hamel, and Michael Ibba

BIOPHYSICS AND COMPUTATIONAL BIOLOGY

3982 **Insight into the mechanism of an iron dioxygenase by resolution of steps following the Fe^{IV}=O species**
Piotr K. Grzyska, Evan H. Appelman, Robert P. Hausinger, and Denis A. Proshlyakov

4016 **Abduction and asylum in the lives of transcription factors**
Anat Burger, Aleksandra M. Walczak, and Peter G. Wolynes

4069 **Markov random fields reveal an N-terminal double beta-propeller motif as part of a bacterial hybrid two-component sensor system**
Matt Menke, Bonnie Berger, and Lenore Cowen

4075 **Ketosteroid isomerase provides further support for the idea that enzymes work by electrostatic preorganization**
Shina C. L. Kamerlin, Pankaz K. Sharma, Zhen T. Chu, and Arieh Warshel

4081 **pH (low) insertion peptide (pHLIP) inserts across a lipid bilayer as a helix and exits by a different path**
Oleg A. Andreev, Alexander G. Karabadzhak, Dhammika Weerakkody, Gregory O. Andreev, Donald M. Engelman, and Yana K. Reshetnyak

4087 **Function and specificity of synthetic Hox transcription factors in vivo**
Dimitrios K. Papadopoulos, Vladana Vukojević, Yoshitsugu Adachi, Lars Terenius, Rudolf Rigler, and Walter J. Gehring

4093 **Quantitative study of synthetic Hox transcription factor–DNA interactions in live cells**
Vladana Vukojević, Dimitrios K. Papadopoulos, Lars Terenius, Walter J. Gehring, and Rudolf Rigler

4099 **The transition state for folding of an outer membrane protein**
Gerard H. M. Huysmans, Stephen A. Baldwin, David J. Brockwell, and Sheena E. Radford
→ *See Commentary on page 3947*

4105 **RNA looping by PTB: Evidence using FRET and NMR spectroscopy for a role in splicing repression**
Rajan Lamichhane, Gerrit M. Daubner, Judith Thomas-Crusells, Sigrid D. Auweter, Cristina Manatschal, Keyunna S. Austin, Oksana Valniuk, Frédéric H.-T. Allain, and David Rueda

4111 **An atomic-level mechanism for activation of the kinesin molecular motors**
Charles V. Sindelar and Kenneth H. Downing
→ *See Commentary on page 3949*

4117 **Heterospecies partition analysis reveals binding curve and stoichiometry of protein interactions in living cells**
Bin Wu, Yan Chen, and Joachim D. Müller

4123 **Independent initiation of primary electron transfer in the two branches of the photosystem I reaction center**
Marc G. Müller, Chavdar Slavov, Rajiv Luthra, Kevin E. Redding, and Alfred R. Holzwarth

4129 **Surface-coupled proton exchange of a membrane-bound proton acceptor**
Tor Sandén, Lina Salomonsson, Peter Brzezinski, and Jerker Widengren

4135 **Electrostatics of aquaporin and aquaglyceroporin channels correlates with their transport selectivity**
Romina Oliva, Giuseppe Calamita, Janet M. Thornton, and Marialuisa Pellegrini-Calace

CELL BIOLOGY

4141 **Membrane curvature controls dynamin polymerization**
Aurélien Roux, Gerbrand Koster, Martin Lenz, Benoît Sorre, Jean-Baptiste Manneville, Pierre Nassoy, and Patricia Bassereau

4147 **Pharmaceutical modulation of canonical Wnt signaling in multipotent stromal cells for improved osteoinductive therapy**
Ulf Krause, Sean Harris, Angela Green, Joni Ylostalo, Suzanne Zeitouni, Narae Lee, and Carl A. Gregory

4153 **ATM signals to TSC2 in the cytoplasm to regulate mTORC1 in response to ROS**
Angela Alexander, Sheng-Li Cai, Jinhee Kim, Adrian Nanez, Mustafa Sahin, Kirsteen H. MacLean, Ken Inoki, Kun-Liang Guan, Jianjun Shen, Maria D. Person, Donna Kusewitt, Gordon B. Mills, Michael B. Kastan, and Cheryl Lyn Walker

4159 **Centromere-localized breaks indicate the generation of DNA damage by the mitotic spindle**
Astrid Alonso Guerrero, Mercedes Cano Gamero, Varvara Trachana, Agnes Fütterer, Cristina Pacios-Bras, Nuria Panadero Díaz-Concha, Juan Cruz Cigudosa, Carlos Martínez-A., and Karel H. M. van Wely

4165 **Transcriptional corepressor TLE1 functions with Runx2 in epigenetic repression of ribosomal RNA genes**
Syed A. Ali, Sayyed K. Zaidi, Jason R. Dobson, Abdul R. Shakoori, Jane B. Lian, Janet L. Stein, Andre J. van Wijnen, and Gary S. Stein

4170 **Structure of sterol aliphatic chains affects yeast cell shape and cell fusion during mating**
Pablo S. Aguilar, Maxwell G. Heiman, Tobias C. Walther, Alex Engel, Dominik Schwudke, Nathan Gushwa, Teymuras Kurzchalia, and Peter Walter

4176 **Two isoforms of human RNA polymerase III with specific functions in cell growth and transformation**
Valérie Haurie, Stéphanie Durrieu-Gaillard, Hélène Dumay-Odelot, Daniel Da Silva, Christophe Rey, Martina Prochazkova, Robert G. Roeder, Daniel Besser, and Martin Teichmann

4182 **Diacylglycerol kinase α mediates HGF-induced Rac activation and membrane ruffling by regulating atypical PKC and RhoGDI**
Federica Chianale, Elena Rainero, Cristina Cianflone, Valentina Bettio, Andrea Pighini, Paolo E. Porporato, Nicoletta Filigheddu, Guido Serini, Fabiola Sinigaglia, Gianluca Baldanzi, and Andrea Graziani

4188 **Amyloidogenic light chains induce cardiomyocyte contractile dysfunction and apoptosis via a non-canonical p38α MAPK pathway**
Jianru Shi, Jian Guan, Bingbing Jiang, Daniel A. Brenner, Federica del Monte, Jennifer E. Ward, Lawreen H. Connors, Douglas B. Sawyer, Marc J. Semigran, Thomas E. Macgillivray, David C. Seldin, Rodney Falk, and Ronglih Liao

4194 **Macrophage Wnt7b is critical for kidney repair and regeneration**
Shuei-Liong Lin, Bing Li, Sujata Rao, Eun-Jin Yeo, Thomas E. Hudson, Brian T. Nowlin, Huaying Pei, Lijun Chen, Jie J. Zheng, Thomas J. Carroll, Jeffrey W. Pollard, Andrew P. McMahon, Richard A. Lang, and Jeremy S. Duffield

4200 **Membrane-anchored serine protease matriptase regulates epithelial barrier formation and permeability in the intestine**
Marguerite S. Buzza, Sarah Netzel-Arnett, Terez Shea-Donohue, Aiping Zhao, Chen-Yong Lin, Karin List, Roman Szabo, Alessio Fasano, Thomas H. Bugge, and Toni M. Antalis

4206 **Regulation of synaptic vesicle recycling by complex formation between intersectin 1 and the clathrin adaptor complex AP2**
Arndt Pechstein, Jelena Bacetic, Ardeschir Vahedi-Faridi, Kira Gromova, Anna Sundborger, Nikolay Tomlin, Georg Krainer, Olga Vorontsova, Johannes G. Schäfer, Simen G. Owe, Michael A. Cousin, Wolfram Saenger, Oleg Shupliakov, and Volker Haucke

4212 **N-cadherin ligation, but not Sonic hedgehog binding, initiates Cdo-dependent p38α/β MAPK signaling in skeletal myoblasts**
Min Lu and Robert S. Krauss

DEVELOPMENTAL BIOLOGY

4218 **Regulation of PI3-kinase/Akt signaling by muscle-enriched microRNA-486**
Eric M. Small, Jason R. O'Rourke, Viviana Moresi, Lillian B. Sutherland, John McAnally, Robert D. Gerard, James A. Richardson, and Eric N. Olson

4224 **Spatiotemporal compartmentalization of key physiological processes during muscle precursor differentiation**
Ertuğrul M. Özbudak, Olivier Tassy, and Olivier Pourquié

4230 **Caspase 3/caspase-activated DNase promote cell differentiation by inducing DNA strand breaks**
Brian D. Larsen, Shravanti Rampalli, Leanne E. Burns, Steve Brunette, F. Jeffrey Dilworth, and Lynn A. Megeney

ECOLOGY

4236 **Cycles, phase synchronization, and entrainment in single-species phytoplankton populations**
Thomas M. Massie, Bernd Blasius, Guntram Weithoff, Ursula Gaedke, and Gregor F. Fussmann

ENVIRONMENTAL SCIENCES

4242 **The tolerance–fecundity trade-off and the maintenance of diversity in seed size**
Helene C. Muller-Landau

EVOLUTION

4248 **Fitness flux and ubiquity of adaptive evolution**
Ville Mustonen and Michael Lässig

4254 **Selective loss of polymorphic mating types is associated with rapid phenotypic evolution during morphic speciation**
Ammon Corl, Alison R. Davis, Shawn R. Kuchta, and Barry Sinervo

4260 **Phenotypic plasticity facilitates recurrent rapid adaptation to introduced predators**
Alison G. Scoville and Michael E. Pfrender

GENETICS

3988 **Targeted metabolic labeling of yeast N-glycans with unnatural sugars**
Mark A. Breidenbach, Jennifer E. G. Gallagher, David S. King, Brian P. Smart, Peng Wu, and Carolyn R. Bertozzi

4264 **Natural variation for seed dormancy in Arabidopsis is regulated by additive genetic and molecular pathways**
Leónie Bentsink, Johannes Hanson, Corrie J. Hanhart, Hetty Blankestijn-de Vries, Colin Coltrane, Paul Keizer, Mohamed El-Lithy, Carlos Alonso-Blanco, M. Teresa de Andrés, Matthieu Reymond, Fred van Eeuwijk, Sjef Smeekens, and Maarten Koornneef

4270 **Multilocus tetrasomic linkage analysis using hidden Markov chain model**
Lindsey J. Leach, Lin Wang, Michael J. Kearsey, and Zewei Luo

IMMUNOLOGY

4275 **PD-1 and CTLA-4 combination blockade expands infiltrating T cells and reduces regulatory T and myeloid cells within B16 melanoma tumors**
Michael A. Curran, Welby Montalvo, Hideo Yagita, and James P. Allison

4281 **Dendritic cell targeted HIV gag protein vaccine provides help to a DNA vaccine including mobilization of protective $CD8^+$ T cells**
Godwin Nchinda, David Amadu, Christine Trumpfheller, Olga Mizenina, Klaus Überla, and Ralph M. Steinman

4287 **Mature dendritic cells use endocytic receptors to capture and present antigens**
Craig D. Platt, Jessica K. Ma, Cécile Chalouni, Melanie Ebersold, Hani Bou-Reslan, Richard A. D. Carano, Ira Mellman, and Lélia Delamarre

4293 **TGF-β regulates T-cell neurokinin-1 receptor internalization and function**
Martin Beinborn, Arthur Blum, Long Hang, Tommy Setiawan, Jonathan C. Schroeder, Korynn Stoyanoff, John Leung, and Joel V. Weinstock

MEDICAL SCIENCES

3953 **Vaccination with partial knowledge of external effectiveness**
Charles F. Manski

3966 **Systemic antiangiogenic activity of cationic poly-L-lysine dendrimer delays tumor growth**
Khuloud T. Al-Jamal, Wafa' T. Al-Jamal, Simon Akerman, Jennifer E. Podesta, Açelya Yilmazer, John A. Turton, Alberto Bianco, Neil Vargesson, Chryso Kanthou, Alexander T. Florence, Gillian M. Tozer, and Kostas Kostarelos

4299 **Disruption of angiogenesis and tumor growth with an orally active drug that stabilizes the inactive state of PDGFRβ/B-RAF**
Eric A. Murphy, David J. Shields, Konstantin Stoletov, Elena Dneprovskaia, Michele McElroy, Joshua I. Greenberg, Jeff Lindquist, Lisette M. Acevedo, Sudarshan Anand, Bharat Kumar Majeti, Igor Tsigelny, Adrian Saldanha, Breda Walsh, Robert M. Hoffman, Michael Bouvet, Richard L. Klemke, Peter K. Vogt, Lee Arnold, Wolfgang Wrasidlo, and David A. Cheresh

4305 **Islet amyloid deposition limits the viability of human islet grafts but not porcine islet grafts**
K. J. Potter, A. Abedini, P. Marek, A. M. Klimek, S. Butterworth, M. Driscoll, R. Baker, M. R. Nilsson, G. L. Warnock, J. Oberholzer, S. Bertera, M. Trucco, G. S. Korbutt, P. E. Fraser, D. P. Raleigh, and C. B. Verchere

4311 **Activatable cell penetrating peptides linked to nanoparticles as dual probes for in vivo fluorescence and MR imaging of proteases**
Emilia S. Olson, Tao Jiang, Todd A. Aguilera, Quyen T. Nguyen, Lesley G. Ellies, Miriam Scadeng, and Roger Y. Tsien

4317 **Surgery with molecular fluorescence imaging using activatable cell-penetrating peptides decreases residual cancer and improves survival**
Quyen T. Nguyen, Emilia S. Olson, Todd A. Aguilera, Tao Jiang, Miriam Scadeng, Lesley G. Ellies, and Roger Y. Tsien

4323 **High-risk neuroblastoma tumors with 11q-deletion display a poor prognostic, chromosome instability phenotype with later onset**
Helena Carén, Hanna Kryh, Maria Nethander, Rose-Marie Sjöberg, Catarina Träger, Staffan Nilsson, Jonas Abrahamsson, Per Kogner, and Tommy Martinsson

4329 **Loss of myeloid cell-derived vascular endothelial growth factor accelerates fibrosis**
Christian Stockmann, Yann Kerdiles, Marc Nomaksteinsky, Alexander Weidemann, Norihiko Takeda, Andrew Doedens, Antonio X. Torres-Collado, Luisa Iruela-Arispe, Victor Nizet, and Randall S. Johnson

4335 **Neural differentiation of human induced pluripotent stem cells follows developmental principles but with variable potency**
Bao-Yang Hu, Jason P. Weick, Junying Yu, Li-Xiang Ma, Xiao-Qing Zhang, James A. Thomson, and Su-Chun Zhang

MICROBIOLOGY

4341 **Only two amino acids are essential for cytolytic toxin recognition of cholesterol at the membrane surface**
Allison J. Farrand, Stephanie LaChapelle, Eileen M. Hotze, Arthur E. Johnson, and Rodney K. Tweten

4347 **Three-dimensional structure of tropism-switching *Bordetella* bacteriophage**
Wei Dai, Asher Hodes, Wong H. Hui, Mari Gingery, Jeff F. Miller, and Z. Hong Zhou

4353 **Gallstones play a significant role in *Salmonella* spp. gallbladder colonization and carriage**
Robert W. Crawford, Roberto Rosales-Reyes, María de la Luz Ramírez-Aguilar, Oscar Chapa-Azuela, Celia Alpuche-Aranda, and John S. Gunn

4359 **Reactogenicity of live-attenuated *Vibrio cholerae* vaccines is dependent on flagellins**
Haopeng Rui, Jennifer M. Ritchie, Roderick T. Bronson, John J. Mekalanos, Yuanxing Zhang, and Matthew K. Waldor

4365 **In vivo actin cross-linking induced by *Vibrio cholerae* type VI secretion system is associated with intestinal inflammation**
Amy T. Ma and John J. Mekalanos

4371 **Molecular complexity of successive bacterial epidemics deconvoluted by comparative pathogenomics**
Stephen B. Beres, Ronan K. Carroll, Patrick R. Shea, Izabela Sitkiewicz, Juan Carlos Martinez-Gutierrez, Donald E. Low, Allison McGeer, Barbara M. Willey, Karen Green, Gregory J. Tyrrell, Thomas D. Goldman, Michael Feldgarden, Bruce W. Birren, Yuriy Fofanov, John Boos, William D. Wheaton, Christiane Honisch, and James M. Musser

4377 **Molecular keys of the tropism of integration of the cholera toxin phage**
Bhabatosh Das, Julien Bischerour, Marie-Eve Val, and François-Xavier Barre
→ *See Commentary on page 3951*

4383 **The early autophagic pathway is activated by hepatitis B virus and required for viral DNA replication**
Donna Sir, Yongjun Tian, Wen-ling Chen, David K. Ann, Tien-Sze Benedict Yen, and Jing-hsiung James Ou

NEUROSCIENCE

4389 **Promoting social behavior with oxytocin in high-functioning autism spectrum disorders**
Elissar Andari, Jean-René Duhamel, Tiziana Zalla, Evelyn Herbrecht, Marion Leboyer, and Angela Sirigu

4395 **BDNF variant Val66Met interacts with estrous cycle in the control of hippocampal function**
Joanna L. Spencer, Elizabeth M. Waters, Teresa A. Milner, Francis S. Lee, and Bruce S. McEwen

4401 **Forebrain overexpression of CK1δ leads to down-regulation of dopamine receptors and altered locomotor activity reminiscent of ADHD**
Mingming Zhou, Heike Rebholz, Christine Brocia, Jennifer L. Warner-Schmidt, Allen A. Fienberg, Angus C. Nairn, Paul Greengard, and Marc Flajolet

4407 **Lower number of cerebellar Purkinje neurons in psychosis is associated with reduced reelin expression**
Ekrem Maloku, Ignacio R. Covelo, Ingeborg Hanbauer, Alessandro Guidotti, Bashkim Kadriu, Qiaoyan Hu, John M. Davis, and Erminio Costa

4412 **Endocytosis and clathrin-uncoating defects at synapses of auxilin knockout mice**
Yang-In Yim, Tao Sun, Ling-Gang Wu, Andrea Raimondi, Pietro De Camilli, Evan Eisenberg, and Lois E. Greene

4418 **Molecular basis of odor coding in the malaria vector mosquito *Anopheles gambiae***
Guirong Wang, Allison F. Carey, John R. Carlson, and Laurence J. Zwiebel

4424 **Genetic approach for intracerebroventricular delivery**
Limor Regev, Eli Ezrielev, Eran Gershon, Shosh Gil, and Alon Chen

4430 **Cortical activity during motor execution, motor imagery, and imagery-based online feedback**
Kai J. Miller, Gerwin Schalk, Eberhard E. Fetz, Marcel den Nijs, Jeffrey G. Ojemann, and Rajesh P. N. Rao

4436 **Adult hippocampal neurogenesis is functionally important for stress-induced social avoidance**
Diane C. Lagace, Michael H. Donovan, Nathan A. DeCarolis, Laure A. Farnbauch, Shveta Malhotra, Olivier Berton, Eric J. Nestler, Vaishnav Krishnan, and Amelia J. Eisch

PHARMACOLOGY

4442 **Morphine peripheral analgesia depends on activation of the PI3Kγ/AKT/nNOS/NO/K_{ATP} signaling pathway**
Thiago M. Cunha, Danilo Roman-Campos, Celina M. Lotufo, Hugo L. Duarte, Guilherme R. Souza, Waldiceu A. Verri, Jr., Mani I. Funez, Quintino M. Dias, Ieda R. Schivo, Andressa C. Domingues, Daniela Sachs, Silvana Chiavegatto, Mauro M. Teixeira, John S. Hothersall, Jader S. Cruz, Fernando Q. Cunha, and Sergio H. Ferreira

4448 **IL-33 augments substance P–induced VEGF secretion from human mast cells and is increased in psoriatic skin**
Theoharis C. Theoharides, Bodi Zhang, Duraisamy Kempuraj, Michael Tagen, Magdalini Vasiadi, Asimenia Angelidou, Konstantinos-Dionysios Alysandratos, Dimitris Kalogeromitros, Shahrzad Asadi, Nikolaos Stavrianeas, Erika Peterson, Susan Leeman, and Pio Conti

4454 **Salt bridge integrates GPCR activation with protein trafficking**
Jo Ann Janovick and P. Michael Conn

PHYSIOLOGY

4459 **Operation of the voltage sensor of a human voltage- and Ca^{2+}-activated K^+ channel**
Antonios Pantazis, Vadym Gudzenko, Nicoletta Savalli, Daniel Sigg, and Riccardo Olcese

4465 **Cellular in vivo imaging reveals coordinated regulation of pituitary microcirculation and GH cell network function**
Chrystel Lafont, Michel G. Desarménien, Mathieu Cassou, François Molino, Jérôme Lecoq, David Hodson, Alain Lacampagne, Gérard Mennessier, Taoufik El Yandouzi, Danielle Carmignac, Pierre Fontanaud, Helen Christian, Nathalie Coutry, Marta Fernandez-Fuente, Serge Charpak, Paul Le Tissier, Iain CAF Robinson, and Patrice Mollard

4471 **Thyroid hormone exerts negative feedback on hypothalamic type 4 melanocortin receptor expression**
Stéphanie Decherf, Isabelle Seugnet, Soumaya Kouidhi, Alejandra Lopez-Juarez, Marie-Stéphanie Clerget-Froidevaux, and Barbara A. Demeneix

PLANT BIOLOGY

4477 **Nitrate-responsive miR393/*AFB3* regulatory module controls root system architecture in *Arabidopsis thaliana***
Elena A. Vidal, Viviana Araus, Cheng Lu, Geraint Parry, Pamela J. Green, Gloria M. Coruzzi, and Rodrigo A. Gutiérrez

PSYCHOLOGICAL AND COGNITIVE SCIENCES

4483 **Innate sensitivity for self-propelled causal agency in newly hatched chicks**
Elena Mascalzoni, Lucia Regolin, and Giorgio Vallortigara

CORRECTIONS

BIOPHYSICS AND COMPUTATIONAL BIOLOGY

4486 **How sequence defines structure: A crystallographic map of DNA structure and conformation**
Franklin A. Hays, Amy Teegarden, Zebulon J. R. Jones, Michael Harms, Dustin Raup, Jeffrey Watson, Emily Cavaliere, and P. Shing Ho

NEUROSCIENCE

4486 **Patterns of neural activity associated with honest and dishonest moral decisions**
Joshua D. Greene and Joseph M. Paxton

ix Author Index

xii Subscription Form

March 2, 2010 | vol. 107 | no. 9 | 3943–4486

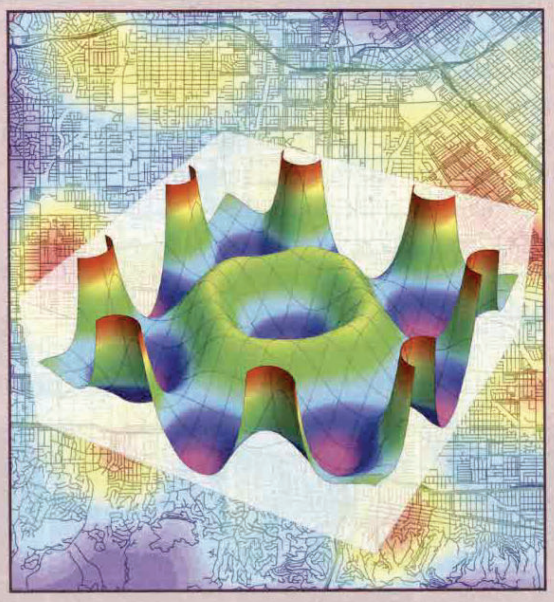
PNAS

Proceedings of the National Academy of Sciences of the United States of America www.pnas.org

In This Issue

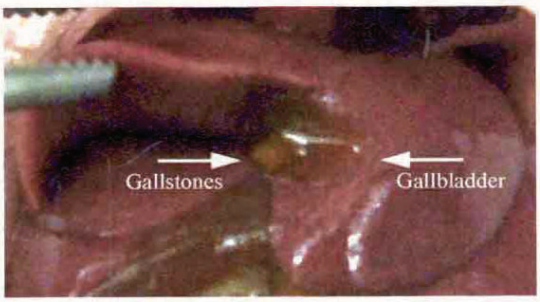
Mathematicians differentiate crime hotspots

Previous research has shown that focusing police resources in crime "hotspots," high-risk locations within communities, can reduce the number of criminal offenses at that location. But predicting whether this strategy can suppress criminal activity, or whether the action simply displaces crime into adjacent areas, is less well understood. In an attempt to coordinate crime-prevention strategies with mapped crime patterns, Martin Short et al. (pp. 3961–3965) devised a pair of coupled differential equations to simulate how criminals search for and choose their targets. According to the authors, the equations constitute a mechanistic model that may reproduce how crime tends to cluster geographically over time. By examining numerous computer simulations, the authors claim that when crime "spikes" in communities with higher-than-average crime rates, a focused police response can eradicate the hotspots permanently. Small fluctuations in criminal activity in locations with lower-than average crime rates, on the other hand, are more likely to result in crime displacement by hotspot policing. The model may aid police forces by predicting where short-term increases in police presence are most likely to produce lasting results. — T.J.



Effects of hotspot policing superimposed on burglary hotspots in Los Angeles, CA.

Gallstones and typhoid in mice and men



Cholesterol diet-induced gallstones in the gallbladder of experimental mice.

Typhoid-inducing salmonella bacteria, *Salmonella* Typhi, may hide from the body's immune defenses and resist clinical treatment by forming biofilms on cholesterol gallstones. *S.* Typhi is well-adapted to the human gallbladder, despite the organ's bile-rich environment, and commonly persists in the body after acute typhoid symptoms subside. In patients carrying *S.* Typhi and gallstones, clinically administered antibiotics typically prove ineffective against the bacterial infection, and removal of the gallbladder remains the most successful treatment option. Robert Crawford et al. (pp. 4353–4358) report that mice inoculated with Typhimurium and fed high cholesterol diets formed biofilm-covered gallstones, and harbored a larger number of bacteria in the gallbladder tissue, bile, and fecal matter than gallstone-free mice. The authors also tested excised gallstones from patients found to be asymptomatic typhoid carriers, and observed 80–95% *S.* Typhi biofilm coverage on all but one sample. The researchers suggest that *S.* Typhi biofilm formation on cholesterol gallstones may help to explain the disease's asymptomatic persistence and spread. The research may facilitate further investigations into the genetics and molecular biology of *S.* Typhi carriage in vivo, and implies an additional therapeutic target against the spread of typhoid fever, according to the authors. — J.M.

Oxytocin and autism

Despite their preserved intellectual function, patients who suffer from Asperger syndrome and other high-functioning autism spectrum disorders typically do not engage appropriately with others in social situations. Previous research has shown that oxytocin, a hormone active in social behaviors and emotions, is deficient in some children with autism. Elissar Andari et al. (pp. 4389–4394) report that administering oxytocin to high-functioning autism patients appears to promote social behavior. The authors administered oxytocin via inhalation to 13 patients with high-functioning autism disorders and confirmed the hormone's distribution by measuring the patients' blood

Author Index

MARCH 9, 2010

A

Adame, L. 4612
Adelstein, J. S. 4734
Adler, D. 4596
Adolphs, R. 4705
Akbudak, E. 4728
Alizadeh, T. 4555
Alphey, L. 4550
An, K. 4710
Anchan, R. M. 4596
Andreolli, G. 4758
Andres, C. 4782
Ansari, A. Z. 4544
Arnold, N. 4505
Austin, A. T. 4618
Aw, D. 4550

B

Babar, I. 4693
Bailey, C. H. 4710
Bailey, J. R. 4693
Baker, J. T. 4728
Baldoli, C. 4758
Ballaré, C. L. 4618
Barry, W. T. 4693
Bauer, S. 4505
Baxter, N. J. 4555
Beckmann, C. F. ... 4734
Beekman, M. 4607
Bell, C. D. 4623
Benoist, C. 4658
Berendonk, T. U. 4550
Bergman, R. N. 4770
Berkowitz, D. B. ... 4555
Bhimsaria, D. 4544
Binder, J. B. 4516
Biswal, B. B. 4734
Blackburn, G. M. 4555
Bouche, C. 4770
Bowler, M. W. 4555
Bowman, G. 4681
Box, A. C. 4640
Brennan, M. P. 4669
Breuer, C. K. 4669
Brown, T. 4612
Brune, N. 4746
Brust, P. 4746
Buchholz, D. 4612
Buckner, R. L. 4734
Burleigh, J. G. 4623

C

Carlson, C. D. 4544
Carmody, A. 4693
Casal, J. J. 4776
Cashmore, A. R. 4499
Castellanos, F. X. 4734
Castro, M. G. 4716
Cerdán, P. D. 4776
Cerrina, F. 4544
Chan, E. 4612
Chan, R. J. 4573
Choi, Y.-B. 4710
Christen, B. 4681
Chu, J. 4579
Chumachenko, N. V. 4585
Cliff, M. J. 4555
Colcombe, S. 4734
Colom, R. 4705
Corbetta, M. 4728
Crawford, A. R. ... 4675
Cui, Y. 4489
Culver, G. M. 4567
Cypess, A. M. 4770

D

Damasio, H. 4705
Dang, Y. 4764
Dawson, T. E. 4533
DeLeo, F. R. 4693
Demirci, U. 4596
Devine, L. 4669
DeYoung, M. P. ... 4675
Ditschun, T. 4746
Dogonowski, A.-M. 4734
D'Souza, P. 4722
Dong, J. 4539
DuBois, G. E. 4746
Durrett, R. 4491
Dussutour, A. 4607

E

Egelman, E. H. 4590
Ellisen, L. W. 4675
Elsaesser, R. 4740
Ernst, M. 4734

F

Fair, D. 4734
Fang, C.-M. 4664
Fero, M. J. 4681
Fine, R. M. 4752
Fleischman, A. 4770
Franzblau, S. G. ... 4573
Fu, G. 4550
Fu, X. 4579

G

Galkin, V. E. 4590
Gallipeau, S. 4612
García-Morales, V. 4528
Gardner, D. J. 4693
Gläscher, J. 4705
Gohel, S. 4734
Goldfine, A. B. 4770
Goldschmidt-Clermont, M. 4782
Graham, M. R. 4693
Gray, P. 4550
Gu, W. 4579
Guo, F. 4640

H

Hahnloser, R. H. R. 4722
Hampson, M. 4734
Hatta, M. 4687
Hauschild, K. E. ... 4544
Hayes, T. B. 4612
He, Y. 4573
Hibino, N. 4669
Hillson, N. J. 4681
Hinz, J. M. 4646
Hong, S.-H. 4681
Hoptman, M. J. ... 4734
Horak, P. 4675
Hounslow, A. M. 4555
Hu, L. 4699
Huang, H. 4658
Hui, M. P. 4590
Huso, D. 4664
Hyde, J. S. 4734

I

Iida, Y. 4601
Ingelsson, B. 4782
Ireland, R. M. 4693

J

J. Siegle, G. 4734
James, A. A. 4550
Jasinskiene, N. 4550
Java, A. 4746
Jay, S. M. 4669
Jeong, A. Y. 4710
Jin, L. 4550
Johnson, C. A. 4693
Johnstone, J. A. ... 4533
Jordan, K. R. 4652, 4788
Jung, J. H. 4710
Jung, S.-Y. 4710
Jung, S. Y. 4579

K

Kahn, C. R. 4770
Kalra, D. 4740
Kaltenbrunner, M. 4505
Kamdar, P. 4746
Kandel, E. R. 4710
Kappler, J. W. 4652
Kappler,, J. W. 4788
Karanewsky, D. S. 4746
Kawaoka, Y. 4687
Kayaalp, E. 4596
Kelly, C. 4734
Kemmler, C. B. 4652, 4788
Keplinger, C. 4505
Kessler, F. 4782
Khoury, V. 4612
Kim Phuc, H. 4550
Kim, J.-H. 4710
Kim, J. 4710
Kirthi, N. 4567
Kiviniemi, V. J. 4734
Klebansky, B. 4752
Kobayashi, S. D. ... 4693
Koelsch, S. 4758
Kötter, R. 4734
Krischer, K. 4528
Kulkarni, R. N. 4770
Kupko 3rd, J. J. ... 4693
Kuscsik, Z. 4511
Kwon, O. B. 4710
Kyriakides, T. R. 4669

L

Lartillot, N. 4629
Latty, T. 4607
Le Men, J. 4640
Lee, C. J. 4710
Lee, Y. 4544
Lees, R. S. 4550
Li, C. 4687
Li, J. 4522
Li, M. 4579
Li, R. 4740
Li, S.-J. 4734
Li, X. 4746, 4752
Lien, C. 4664
Lin, C.-P. 4734
Liu, H. 4752
Liu, J.-G. 4511
Liu, J. O. 4764
Liu, L. 4699
Liu, S.-C. 4722
Liu, S. 4579
Liu, Y. 4573
Liu, Y.-L. 4522
Livak, F. 4664
Lopez, X. 4770
Lowe, M. J. 4734
Lowenstein, P. R. .. 4716
Lu, R. 4664
Luo, Y. 4573

M

Maas, R. L. 4596
Mackay, C. 4734
Madden, D. J. 4734
Madsen, K. H. 4734
Mak, H. Y. 4640
Margulies, D. S. ... 4734
Marinotti, O. 4550
Mathis, D. 4658
Mayberg, H. S. 4734
McAdams, H. H. 4681
McMahan, R. H. 4652, 4788
McMahon, K. 4734
Medo, M. 4511
Mennes, M. 4734
Milham, M. P. 4734
Mirensky, T. L. 4669
Miura, M. 4601
Monk, C. S. 4734
Montell, C. 4740
Moore, M. J. 4623
Mostofsky, S. H. ... 4734
Mu, J.-J. 4579
Muramoto, Y. 4687
Musser, J. M. 4693

N

Nagel, B. J. 4734
Nalbandian, A. 4669
Narayan, A. 4612
Nash, Z. M. 4675
Nazir, M. 4612
Neumann, G. 4687
Nidom, C. A. 4687
Nilges, M. J. 4522
Nimmo, D. 4550
No, J.-H. 4522
Nureddin, A. 4596

O

Oldfield, E. 4522
O'Malley, B. W. ... 4579
O'Shea, S. 4770
Ozers, M. S. 4544

P

Park, A. 4612
Parnell, M. J. 4693
Patel, G. H. 4728
Paul, L. K. 4705
Pekar, J. J. 4734
Peltier, S. J. 4734
Perani, D. 4758
Petersen, S. E. 4734
Petrovic, G. 4746
Philippe, H. 4629

Pitha, P. M. 4664
Pober, J. S. 4669
Porcella, S. F. 4693
Puntel, M. 4716

Q

Qadir, N. 4544
Qin, J. 4579

R

Raines, R. T. 4516
Rao, D. A. 4669
Ren, Y. R. 4764
Ricklefs, S. M. 4693
Riedl, V. 4734
Rochaix, J.-D. 4782
Rodrigue, N. 4629
Rodriguez, Y. 4646
Rogatsky, E. 4770
Roh, J. D. 4669
Rombouts, S. A. R. B. 4734
Rovelli, R. 4758
Roy-Chaudhuri, B. 4567
Rudrauf, D. 4705
Rypma, B. 4734

S

Saccuman, M. C. 4758
Saltzman, W. M. 4669
Samol, I. 4782
Sánchez-Lamas, M. 4776
Sanderson, N. S. R. 4716
Sawh-Martinez, R. 4669
Scaife, S. 4550
Schlaggar, B. L. ... 4734
Schmidt, S. 4734
Scifo, P. 4758
Seidler, R. D. 4734
Servant, G. 4746, 4752
Sgroi, D. 4675
Shao, F. 4699
Shapiguzov, A. 4782
Shapiro, L. 4681
Shattuck, M. R. ... 4635
Shea, P. R. 4693
Shinoka, T. 4669
Shulman, G. L. ... 4728
Siegle, G. J. 4734
Simpson, S. J. 4607
Slansky, J. E. 4652, 4788
Smerdon, M. J. ... 4646
Smith, S. M. 4734
Snyder, A. Z. 4728
Snyder, E. 4669
Snyder, L. H. 4728
Soltis, D. E. 4623
Soltis, P. S. 4623
Song, Y. S. 4596
Sorg, C. 4734
Spada, D. 4758
Stasiak, A. 4590
Stasiak, A. Z. 4590
Stefanovski, D. ... 4770
Stein, D. T. 4770
Strasser, B. 4776
Stueve, T. 4612
Sturdevant, D. E. 4693

T

Tachdjian, C. 4746, 4752
Tang, X.-Q. 4746
Tang, X. 4539
Teng, G.-J. 4734
Tomooka, Y. 4601
Tranel, D. 4705
Trimble, R. 4640
Turk, R. M. 4585

U

Udelsman, B. 4669
Umezu, T. 4601

V

Vadysirisack, D. D. 4675
Veijola, J. 4734
Vener, A. V. 4782
Villringer, A. 4734
Virtaneva, K. 4693

W

Wakeling, J. R. ... 4511
Waldor, M. K. 4590
Walter, M. 4734
Waltho, J. P. 4555
Wang, K. 4522
Wang, L. 4734
Wang, W. 4522
Wang, Y. 4573, 4579
Warren, C. L. 4544
Watanabe, S. 4687
Wawrowsky, K. ... 4716
Wells, J. A. 4561
Weng, X.-C. 4734
Werner, S. 4746
White-Cooper, H. 4550
Whitfield-Gabrieli, S. 4734
Wildes, D. 4561
Williams, N. H. ... 4555
Williams, S. A. ... 4635
Williamson, P. 4734
Windischberger, C. 4734
Wright, F. A. 4693
Wu, B. 4555

X

Xie, C. 4489
Xu, F. 4596
Xu, H. 4752
Xu, J. 4573, 4764
Xu, N. 4640

Y

Yamanouchi, H. 4601
Yang, J. 4716
Yang, T. 4579
Yang, Z. 4573
Yanovsky, M. J. 4776
Yao, Q. 4699
Yarus, M. 4585
Yi, P. 4579
Yi, T. 4669
Yu, J. 4640
Yu, X. 4590
Yucer, N. 4579

Z

Zang, Y.-F. 4734
Zhang, F. 4746, 4752
Zhang, H.-Y. 4734
Zhang, S. O. 4640
Zhang, X. 4573
Zhang, Y.-C. 4511
Zhang, Z.-Y. 4573
Zheng, J. 4573
Zhou, B. 4573
Zhou, T. 4511
Zhou, Y. 4699
Zhu, Y. 4699
Zoller, M. 4746, 4752
Zuo, X.-N. 4734

This material may be protected by Copyright law (Title 17 U.S. Code)

PD-1 and CTLA-4 combination blockade expands infiltrating T cells and reduces regulatory T and myeloid cells within B16 melanoma tumors

Michael A. Curran[a], Welby Montalvo[a], Hideo Yagita[b], and James P. Allison[a,1]

[a]Howard Hughes Medical Institute, Department of Immunology, Memorial Sloan-Kettering Cancer Center, New York, NY 10065; and [b]Department of Immunology, Juntendo University School of Medicine, 2-1-1 Hongo, Bunkyo-ku, Tokyo 113-8421, Japan

Contributed by James P. Allison, January 19, 2010 (sent for review December 17, 2009)

Vaccination with irradiated B16 melanoma cells expressing either GM-CSF (Gvax) or Flt3-ligand (Fvax) combined with antibody blockade of the negative T-cell costimulatory receptor cytotoxic T-lymphocyte antigen-4 (CTLA-4) promotes rejection of preimplanted tumors. Despite CTLA-4 blockade, T-cell proliferation and cytokine production can be inhibited by the interaction of programmed death-1 (PD-1) with its ligands PD-L1 and PD-L2 or by the interaction of PD-L1 with B7-1. Here, we show that the combination of CTLA-4 and PD-1 blockade is more than twice as effective as either alone in promoting the rejection of B16 melanomas in conjunction with Fvax. Adding αPD-L1 to this regimen results in rejection of 65% of preimplanted tumors vs. 10% with CTLA-4 blockade alone. Combination PD-1 and CTLA-4 blockade increases effector T-cell (Teff) infiltration, resulting in highly advantageous Teff-to-regulatory T-cell ratios with the tumor. The fraction of tumor-infiltrating Teffs expressing CTLA-4 and PD-1 increases, reflecting the proliferation and accumulation of cells that would otherwise be anergized. Combination blockade also synergistically increases Teff-to-myeloid-derived suppressor cell ratios within B16 melanomas. IFN-γ production increases in both the tumor and vaccine draining lymph nodes, as does the frequency of IFN-γ/TNF-α double-producing $CD8^+$ T cells within the tumor. These results suggest that combination blockade of the PD-1/PD-L1- and CTLA-4-negative costimulatory pathways allows tumor-specific T cells that would otherwise be inactivated to continue to expand and carry out effector functions, thereby shifting the tumor microenvironment from suppressive to inflammatory.

Flt3-ligand | melanoma | PD-L1 | immunotherapy | vaccine

The interaction between the T-cell receptor complex (TCR) and antigenic peptides bound in surface MHC molecules provides the specificity that defines adaptive T-cell immunity. In addition to TCR activation, costimulation via ligation of the coreceptor CD28 on T cells by B7 molecules on antigen-presenting cells (APCs) is required for optimal T-cell activation (1). Once mobilized, however, T cells begin to express other members of the CD28/B7 receptor family that attenuate the immune response through inhibition of proliferation and cytokine production (2). Cytotoxic T-lymphocyte antigen-4 (CTLA-4) is rapidly up-regulated following T-cell activation and binds to B7 molecules with a higher affinity than does CD28. The receptor programmed death-1 (PD-1) is also expressed on T cells following activation, where, on binding to its ligands PD-L1 and PD-L2, it promotes T-cell anergy, apoptosis, and exhaustion. Recently, an additional coinhibitory ligand/receptor interaction has been described that involves binding of PD-L1 on T cells to B7-1 on APCs or vice versa (3). Although the existence of so many layers of T-cell inhibition may seem surprising, the severe and sometimes fatal autoimmunity that results when even one of these pathways is disrupted attests to their necessity.

Malignant transformation was classically defined by the ability to avoid the normal regulatory mechanisms of cell growth, division, and death. Another common feature uniting all lineages of tumor is the ability to evade destruction by the host immune system. Ample evidence now exists that T cells infiltrating tumors can be inhibited by both CTLA-4 and PD-1 coinhibitory signals. Myeloid-derived suppressor cells (MDSCs) populating the tumor microenvironment can express both B7-1 and PD-L1 (4). In addition, tumors themselves sometimes express PD-L1, which can negatively signal T cells through both the PD-1 and B7-1 molecules on their surface (5). Antibody blockade of CTLA-4 or PD-1 has been shown to enhance antitumor immune responses in both murine preclinical models and clinical trials (2, 5).

Previously, we have shown that vaccination with B16-GM-CSF (Gvax) or B16-Flt3-ligand (Fvax) promotes the rejection of preimplanted B16-BL6 melanomas when combined with antibody blockade of CTLA-4 (6, 7). Although CTLA-4 and PD-1 belong to the same family of molecules and are both coinhibitory, evidence suggests they use distinct nonredundant mechanisms to inhibit T-cell activation. Most strikingly, CTLA-4 knockout mice die by 4 weeks of age from a lethal lymphoproliferative disorder, whereas some colonies of PD-1 knockout BL6 mice live over a year before manifesting lupus-like symptoms with ~50% penetrance (8, 9). Although the phosphatases Src homology 2-containing tyrosine phosphatase (SHP)-1 and SHP-2 have been implicated in both CTLA-4 and PD-1 negative signaling, the phosphatase PP2A binds only CTLA-4 and leads to inhibition of Akt phosphorylation through a pathway that is distinct from that of PD-1 (10). Also, both PD-1/PD-L1 and CTLA-4/B7 interactions help to maintain peripheral tolerance through modifications in T-cell motility; however, they seem to do so through distinct mechanisms (11, 12). Because the CTLA-4 and PD-1 inhibitory pathways appeared to be nonredundant, we investigated whether PD-1 blockade in addition to CTLA-4 blockade could further enhance rejection of B16 melanoma.

Here, we show that in a B16 melanoma treatment setting in which Fvax + αCTLA-4 cures only 10% of animals, Fvax + αPD-1 promotes tumor rejection in almost 25% of animals. More strikingly, combination blockade of PD-1 and CTLA-4 leads to rejection of 50% of melanomas, and the further addition of αPD-L1 allows 65% of mice to survive tumor-free. We show that blockade of single negative costimulatory pathways often leads to enhanced effector T-cell (Teff) infiltration of tumors but that these T cells accumulate high levels of the unblocked negative coreceptors that eventually limit their expansion. Blockade of multiple coinhibitory pathways allows $CD8^+$ and $CD4^+$ T cells to continue to survive, proliferate, and carry out effector functions

Author contributions: M.A.C. and J.P.A. designed research; M.A.C. and W.M. performed research; M.A.C. and H.Y. contributed new reagents/analytic tools; M.A.C. and J.P.A. analyzed data; and M.A.C. wrote the paper.

Conflict of interest statement: J.P.A. is a paid consultant for Bristol-Myers Squibb and is the primary inventor on the patent "Blockade of T lymphocyte down-regulation associated with CTLA-4 signaling."

[1]To whom correspondence should be addressed. E-mail: allisonj@mskcc.org.

This article contains supporting information online at www.pnas.org/cgi/content/full/0915174107/DCSupplemental.

within the tumor. Combination blockade of the CTLA-4 and PD-1 pathways also cooperates to increase the ratio of Teffs to both regulatory T cells (Tregs) and MDSCs, thereby reducing suppression and promoting inflammation in the tumor microenvironment. Combination blockade further enhances this inflammatory state by increasing the frequency of IFN-γ and TNF-α double-producing T cells within the tumor and by increasing the proliferation of both $CD8^+$ and $CD4^+$ Teffs relative to Fvax treatment alone. Combination blockade of the PD-1, CTLA-4, and PD-L1 coinhibitory molecules coupled with Fvax vaccination initiates an inflammatory cascade in the tumor microenvironment leading to enhanced Teff infiltration, activation, and cytokine production, thereby antagonizing tumor-induced immune suppression and promoting tumor rejection.

Results

PD-1 Blockade Cooperates with CTLA-4 Blockade and Fvax Vaccination to Promote B16 Melanoma Rejection. Combination vaccination with either Gvax or Fvax and antibody blockade of the coinhibitory receptor CTLA-4 prevent the outgrowth of a majority of 3-day preimplanted B16-BL6 melanomas (6). If vaccination is delayed until 5 days following implantation, the efficacy of this therapy declines substantially. When combined with Fvax, PD-1 blockade alone was more effective than CTLA-4 blockade alone and combination blockade of both coinhibitory pathways was synergistic, promoting full rejection of B16 melanoma in half of the animals (Fig. S1*A*). When combined with Gvax + αCTLA-4 therapy, we found that the addition of PD-1 blockade failed to increase survival or slow tumor growth (Fig. S1*B*).

Because higher levels of B7-1 expression have been reported following vaccination with GM-CSF relative to Flt3-ligand, we asked whether increased B7-1/PD-L1 inhibition might be responsible for the observed discrepancy between Gvax and Fvax (13).

With Fvax, Blockade of CTLA-4/B7, PD-1/PD-L1, and B7-1/PD-L1 Interactions Each Promotes Rejection of B16 Melanoma and Is Additive when Used in Combination. To test the contribution of B7-1/PD-L1 inhibition, we used a high B16 challenge (5×10^4 cells) and vaccination on days 3, 6, and 9. In this setting, no antibody regimen without a cellular vaccine was curative (Fig. S2). Also, neither blockade of any single coinhibitory receptor nor of any combination resulted in greater than 20% survival when combined with Gvax (Fig. 1*A*). In the context of Fvax, however, blockade of either the PD-L1 (8% survival), CTLA-4 (10% survival), or PD-1 (25% survival) receptor demonstrated modest therapeutical benefit (Fig. 1*B*). Combination blockade of CTLA-4 and PD-1 promoted tumor rejection in 50% of mice, whereas the further addition of αPD-L1 elevated the rate of tumor-free survival to 65%.

Combination Blockade of the CTLA-4 and PD-1 Pathways Strongly Increases Both $CD8^+$ T-Cell/Treg and $CD4^+$ Teff/Treg Ratios Within the Tumor. Because there was a clear hierarchy of effect of each costimulatory blocking therapy as well as of the combinations when paired with Fvax, we sought to dissect the effects of each therapy on T-cell infiltration of tumor in this background. Both CTLA-4 and PD-1 blockade strongly increased infiltration of tumor by $CD8^+$ T cells, whereas αPD-L1 blockade alone did so only modestly (Fig. 2*A* and Fig. S3*A*). The combination of CTLA-4 and PD-1 blockade increased $CD8^+$ T-cell infiltration more than CTLA-4 blockade alone. In contrast to CTLA-4 and PD-L1 blockade, PD-1 blockade had little effect on the percentage of tumor-infiltrating lymphocytes (TILs) composed of $CD4^+$ Teffs (Fig. 2*B*); however, PD-1 and CTLA-4 increased absolute numbers of infiltrating $CD4^+$ Teffs to a similar degree (Fig. S3*B*). Combination PD-1/CTLA-4 blockade with or without αPD-L1 increased the percentage of CD4 Teff infiltration to a similar degree to that of αCTLA-4 alone; however, absolute numbers of CD4 Teffs appear to be increased to a greater extent by combination therapy. Anti-CTLA-4 treatment alone or in combination with other coinhibitory blockade decreased the fraction of TILs composed of Tregs (Fig. 2*C*); however, the number of Tregs per cubic millimeter of tumor was not diminished (Fig. S3*C*). PD-1 blockade alone, in contrast, did not decrease the TIL fraction of Tregs and seemed to promote an increase in their absolute numbers.

CTLA-4, PD-1, or PD-L1 blockade increases $CD8^+$ T-cell-to-Treg ratios within the tumor, which we have previously described as being predictive of therapeutical efficacy in the B16 melanoma model (14) (Fig. 2*D*). Combination therapy with CTLA-4 and PD-1 blockade increases CD8/Treg ratios significantly more than αCTLA-4 alone, whereas triple coinhibitory blockade is statistically superior to any individual antibody therapy.

Of the single coinhibitory antibodies, only αCTLA-4 significantly improves CD4 Teff/Treg ratios within the tumor (Fig. 2*E*). The combination of αCTLA-4, αPD-1, and αPD-L1 is superior to any other single or combination therapy in terms of promoting advantageous CD4 Teff/Treg ratios in TILs.

Combination Coinhibitory Pathway Blockade Allows Accumulation of High Percentages of Active T Cells Expressing CTLA-4 and PD-1 that Would Otherwise Be Anergized. We hoped to learn more about the activation state of the tumor-infiltrating T cells by measuring their expression of relevant costimulatory molecules. In the CD4 Teff population, the fraction of CTLA-4-expressing cells was increased by each costimulatory blocking antibody alone and cooperatively by the double- and triple-antibody combinations (Fig. 3*A*). The frequency of PD-1 expression by these cells also increased in response to blockade of each coinhibitory pathway, but this elevation in PD-1 frequency was strongest in response to αCTLA-4 alone or in combination with other agents. The sum of these effects more than doubled the frequency of CTLA-4/PD-1 double-positive $CD4^+$ Teffs in the combination-treated vs. untreated mice.

In the case of $CD8^+$ T cells, CTLA-4 was again up-regulated by blockade of any coinhibitory pathway; however, in this case, αPD-1 alone or in combination with other antibodies produced the greatest increase in CTLA-4 expression (Fig. 3*B*). Blockade of CTLA-4, PD-1, or PD-L1 alone resulted in an increased fraction of $CD8^+$ T cells expressing PD-1. Simultaneous blockade of all three receptors resulted in an even higher frequency of PD-1

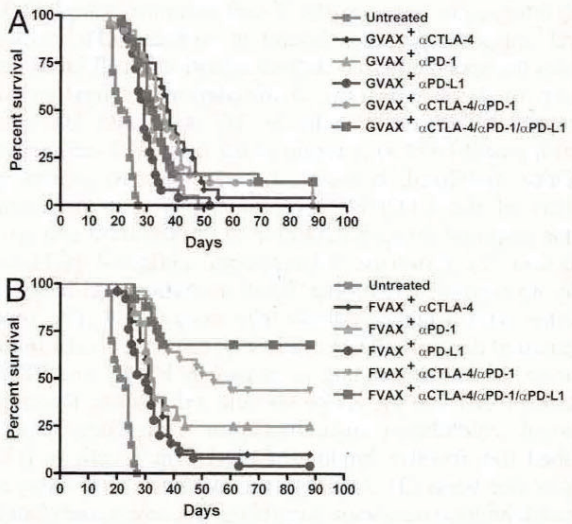


Fig. 1. Survival of mice challenged with 5×10^4 B16-BL6 cells and vaccinated on days 3, 6, and 9 with 1×10^6 Gvax (*A*) or Fvax (*B*) intradermally and the indicated antibody or combination i.p.. Lack of survival was defined as death or tumor size >1,000 mm^3. Each curve represents three to four independent experiments of 5–15 mice per group.

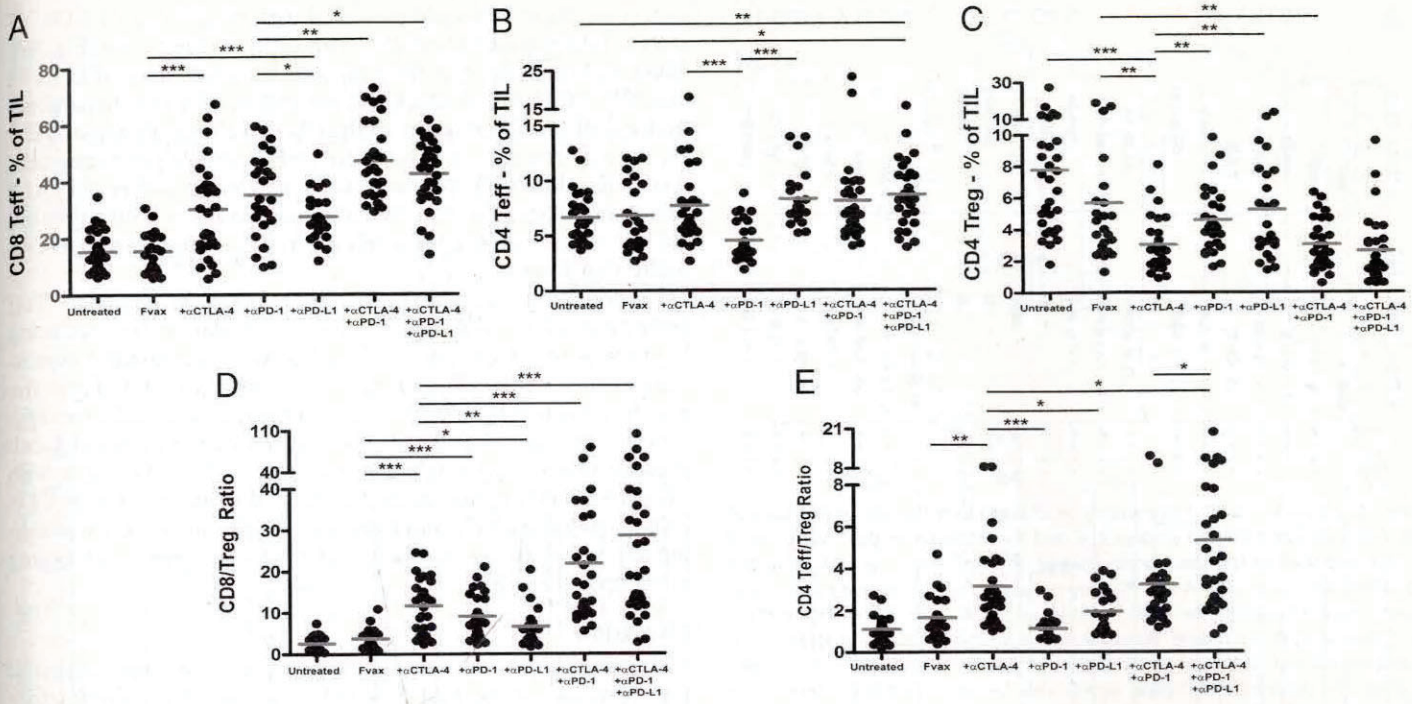


Fig. 2. Lymphocyte infiltration of B16 melanoma. Mice were challenged with 1.5×10^5 B16-BL6 cells; treated with Fvax and the indicated antibody on days 3, 6, and 9; and killed on day 16. Percentages of $CD45^+$ TILs of $CD8^+$ T cells (*A*), $CD4^+$ Teffs (*B*), and Tregs (*C*) are shown. The ratios of $CD8^+$ T cells to Tregs (*D*) and $CD4^+$ Teffs to Tregs (*E*) are shown. Values shown are for individually analyzed mice and are the sum of four to seven independent experiments with 5–15 mice per group. To determine statistical significance between samples, *t* tests were performed. $*P \leq 0.05$; $**P \leq 0.01$; $***P < 0.001$.

expression, with nearly every $CD8^+$ T cell staining positive for PD-1. Vaccination with Fvax combined with any of these antibodies increases the frequency of CTLA-4/PD-1 double-positive $CD8^+$ T cells; however, αPD-1 has a significantly stronger effect than either αCTLA-4 or αPD-L1. Similar to CD4 Teffs, combination costimulatory blockade results in over 75% of $CD8^+$ T cells coexpressing PD-1 and CTLA-4, whereas double-expressing cells make up less than 30% of the $CD8^+$ T cells infiltrating untreated tumors.

Levels of coinhibitory receptor expression were also measured and further demonstrate that blockade of one coinhibitory pathway leads to compensatory up-regulation of others (Fig. S4 *A* and *B*).

Combination Coinhibitory Receptor Blockade Decreases Expression of Treg Activation Markers Except Inducible T-Cell Costimulator (ICOS). CTLA-4 and PD-1, although inhibitory for Teffs, have been implicated in the formation of inducible Tregs as well as in Treg suppressive function, respectively (15, 16). Treatment with αCTLA-4 diminished the rate of CTLA-4 expression by $CD4^+FoxP3^+$ Treg cells, whereas both PD-1 and CTLA-4 blockade reduced the frequency of PD-1 expression (Fig. S5). Combined blockade of PD-1, CTLA-4, and PD-L1 reduced the fraction of intratumoral Tregs expressing CTLA-4 and PD-1 individually as well as the fraction of double-positive cells. In more than a third of triple-combination blockade-treated mice, less than 50% of the Tregs in TILs expressed both CTLA-4 and PD-1, a phenotype not observed in any untreated or Fvax alone-treated animals. Although αCTLA-4 and αPD-1 increased Treg expression levels of the unblocked receptor, both depressed PD-L1 levels when used individually (Fig. S4*C*).

In addition to CTLA-4 and PD-1, expression of 4-1BB and KLRG1 has been associated with enhanced Treg function (17, 18). In each case, we found that combination blockade of the CTLA-4 and PD-1 pathways significantly decreased the fraction of Tregs expressing the relevant activation marker (Fig. S6 *A* and *B*). ICOS expression has also been associated with enhanced Treg function; however, in contrast to the other activation molecules under study, we found that ICOS levels increased on Tregs following treatment with αCTLA-4 or αPD-1 (19) (Fig. S6*C*). Further, simultaneous blockade of both receptors resulted in significantly increased ICOS levels relative to αCTLA-4 alone. Interestingly, αPD-L1 did not promote an increased frequency of $ICOS^{hi}$ $CD4^+$ Tregs when used alone (Fig. S6*C*).

Combination Coinhibitory Receptor Blockade Synergistically Increases the Ratio of Teffs to MDSCs in the Tumor. The activity of the enzyme arginase-1 is an important mechanism by which MDSCs dampen T-cell activity within tumors (4). We assessed the effects of our therapy on MDSCs using both the traditional $CD11b^+GR\text{-}1^+$ gating and a functional $CD11b^+$arginase-1^+ stain. Blockade of either CTLA-4, PD-1, or PD-L1 in the context of Fvax vaccination increased the ratio of $CD8^+$ T cells to MDSCs within the tumor (Fig. 4*A*). Combination blockade of these negative costimulatory receptors synergistically increased CD8/MDSC ratios to more than double those achieved with single coinhibitory blockade and more than 10 times the levels in untreated tumors. Similar results were obtained if MDSCs were defined as $CD11b^+GR\text{-}1^+$ cells (Fig. S7*A*).

CD4 Teff-to-MDSC ($CD11b^+$arginase-1^+) ratios were increased relative to untreated tumor by Fvax + αCTLA-4 vaccination (Fig. 4*B*). As with $CD8^+$ T cells, both double and triple coinhibitory blockade regimens significantly increased the ratio of $CD4^+$ Teffs relative to MDSCs in tumors compared with Fvax treatment alone. Only triple coinhibitory blockade was statistically superior to any single-antibody therapy in this setting. Similar results were obtained if MDSCs were defined as $CD11b^+GR\text{-}1^+$ cells (Fig. S7*B*).

Combination Coinhibitory Receptor Blockade Increases Inflammatory Cytokine Production in the Vaccine and Tumor Draining Lymph Nodes and in the Tumor Itself. To define the functional effects of each therapy on effector cytokine production clearly, we elected to use the B16-ovalbumin (B16-Ova) model antigen system to measure cytokine responses. Mice were challenged with 2.5×10^5 B16-Ova cells in 30% Matrigel (BD Bioscience) and vaccinated

IMMUNOLOGY

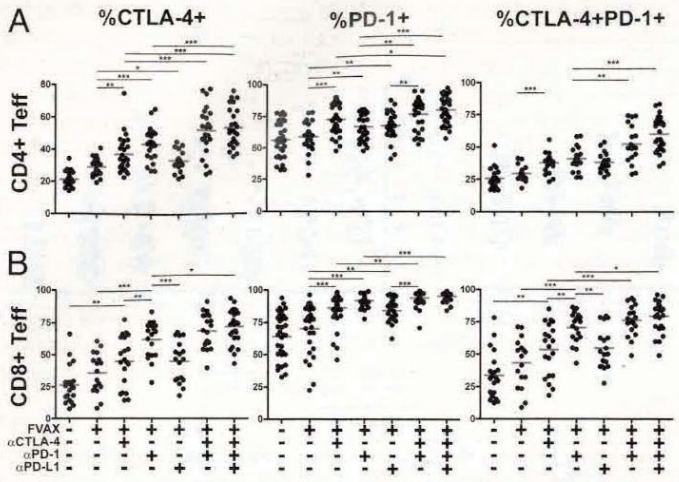


Fig. 3. CTLA-4 and PD-1 expression by TILs. Mice challenged with 1.5×10^5 B16-BL6 cells and treated on days 3, 6, and 9 were killed on day 16. TILs were fixed and stained for lymphocyte lineage and activation markers using the FoxP3 fixation kit. CTLA-4 and PD-1 were stained for surface and intracellular expression. Percentages of $CD8^+$ T cells (*A*) and $CD4^+$ Teffs (*B*) expressing PD-1, CTLA-4, or both are shown. Values shown are for individually analyzed mice and are the sum of three to six independent experiments with 5–15 mice per group. To determine statistical significance between samples, *t* tests were performed. $*P \leq 0.05$; $**P \leq 0.01$; $***P < 0.001$.

on days 6, 9, and 12. Combination costimulatory blockade significantly increased IFN-γ and TNF-α production from CD8 cells in both the vaccine and tumor draining lymph nodes relative to blockade of any single receptor alone (Fig. 5*A*). The addition of PD-L1 blockade to αCTLA-4/αPD-1 combination therapy did not significantly alter inflammatory cytokine production.

$CD4^+$ T cells in the vaccine draining lymph node demonstrated increased IL-10 and IL-4 production with combination costimulatory blockade (Fig. 5*B*). Although this increase reflects the increased activation resulting from PD-1 and CTLA-4 combination blockade, the apparent T helper (Th) 2 polarization likely reflects the known Th2 bias of Ova-specific CD4 responses in this background (20). Despite this Th2 bias, we still observed a significant increase in IFN-γ production in the tumor draining lymph node following CTLA-4 and CTLA-4/PD-1 combination coinhibitory blockade (Fig. 5*B*).

To investigate changes in cytokine expression resulting from combination coinhibitory blockade within the tumor itself further, we restimulated tumor-infiltrating T cells for 8 h with both Ova- and B16 peptide-pulsed dendritic cells (DCs) and measured intracellular cytokine accumulation by flow cytometry. Combination CTLA-4 and PD-1 blockade has previously been associated with increased IFN-γ and TNF-α expression by reactivated $CD8^+$ T cells responding to hepatitis C virus infection (21). Similarly, combination coinhibitory blockade produced high frequencies of $CD8^+$ T cells in TILs producing both IFN-γ and TNF-α (Fig. 5*C* and Fig. S8). Much as we observed in the lymph nodes, addition of αPD-L1 to dual PD-1/CTLA-4 blockade did not significantly enhance inflammatory cytokine production. In the $CD4^+$ Teff population of TILs, the highest fraction of IFN-γ and TNF-α double-producing cells was induced by CTLA-4 blockade alone or in combination with other antibodies (Fig. 5*D*). We also assayed IL-10 production but did not observe substantial levels from any population of B16-Ova infiltrating T cells.

Combination coinhibitory receptor blockade increases Teff infiltration of tumors, and those cells appear to be producing high levels of inflammatory cytokines. We assayed Ki67 expression of tumor-infiltrating T cells in an effort to determine the extent of proliferation of these cells in response to each therapy. CTLA-4 blockade was the strongest driver of intratumoral T-cell proliferation of any single agent tested, and combining it with PD-1 blockade did not further increase division in CD4 or CD8 cells (Fig. 5 *E* and *F*). Intratumoral Treg proliferation was also highest with CTLA-4 blockade alone but was very similar among all samples (Fig. S9).

Discussion

Here, we show that in the context of Fvax vaccination, combination blockade of the CTLA-4- and PD-1-negative costimulatory receptors leads to synergistic levels of tumor rejection. Underlying this effect, we find dramatically enhanced levels of Teff infiltration of tumors and inflammatory cytokine production. The accumulation of CTLA-4/PD-1 double-positive Teffs within B16 melanomas in the context of combination blockade suggests that T cells that would otherwise be functionally and proliferatively repressed are instead able to continue expanding and carrying out effector functions. Addition of PD-L1 blockade to αCTLA-4/αPD-1 combination therapy increased mean survival from 50 to 65% in mice challenged with 5×10^4 B16-BL6 cells. It is unlikely that this represents a direct antitumor effect, because B16 melanoma expresses little to no PD-L1 in vivo (22). The primary benefit of blocking the additional PD-L1/B7-1 inhibitory pathway in this context appeared to be in augmenting the CD4/Treg and CD4/MDSC ratios within B16 melanomas.

It has been shown previously that both CTLA-4 and PD-1 blockade individually augments the capacity of Gvax to promote rejection of B16 melanomas (6, 7, 23). We purposely chose the less immunogenic B16-BL6 model (as opposed to B16-F10) and settings of high tumor challenge or delayed vaccination in hopes of observing cooperative effects between blockade of multiple coinhibitory pathways. Still, we were surprised that even with triple coinhibitory blockade, we were unable to observe any significant additive effects of these antibodies in the context of Gvax. Although we did not pursue the roots of the differences between Fvax and Gvax further, the inability of any T-cell-potentiating antibody combination to promote cure of more than 20% of mice

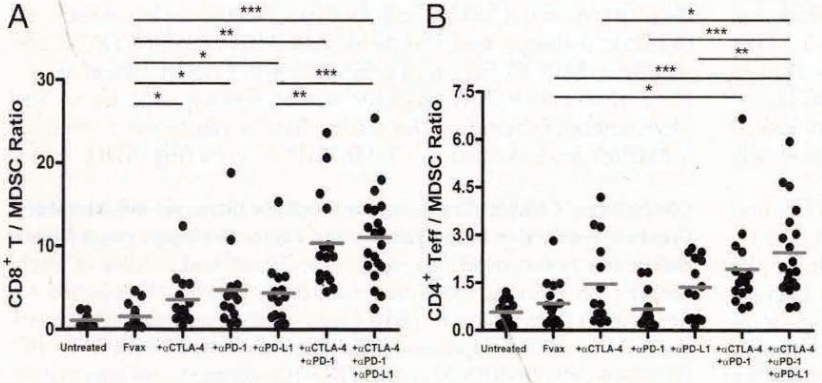


Fig. 4. Ratios of Teffs to MDSCs within tumors. Mice challenged with 1.5×10^5 B16-BL6 cells and treated on days 3, 6, and 9, were killed on day 16. TILs were fixed and stained for lymphocyte and myeloid lineage and activation markers using the FoxP3 fixation kit. Arginase-1 was stained using the 8C9 clone from Santa Cruz. The ratios of $CD8^+$ T cells to $CD11b^+$arginase-1^+ MDSCs (*A*) and $CD4^+$ Teffs to $CD11b^+$arginase-1^+ cells (*B*) within $CD45^+$ melanoma TILs are shown for mice receiving the indicated therapy. Values shown are for individually analyzed mice and are the sum of three independent experiments with 5–15 mice per group. To determine statistical significance between samples, *t* tests were performed. $*P \leq 0.05$; $**P \leq 0.01$; $***P < 0.001$.

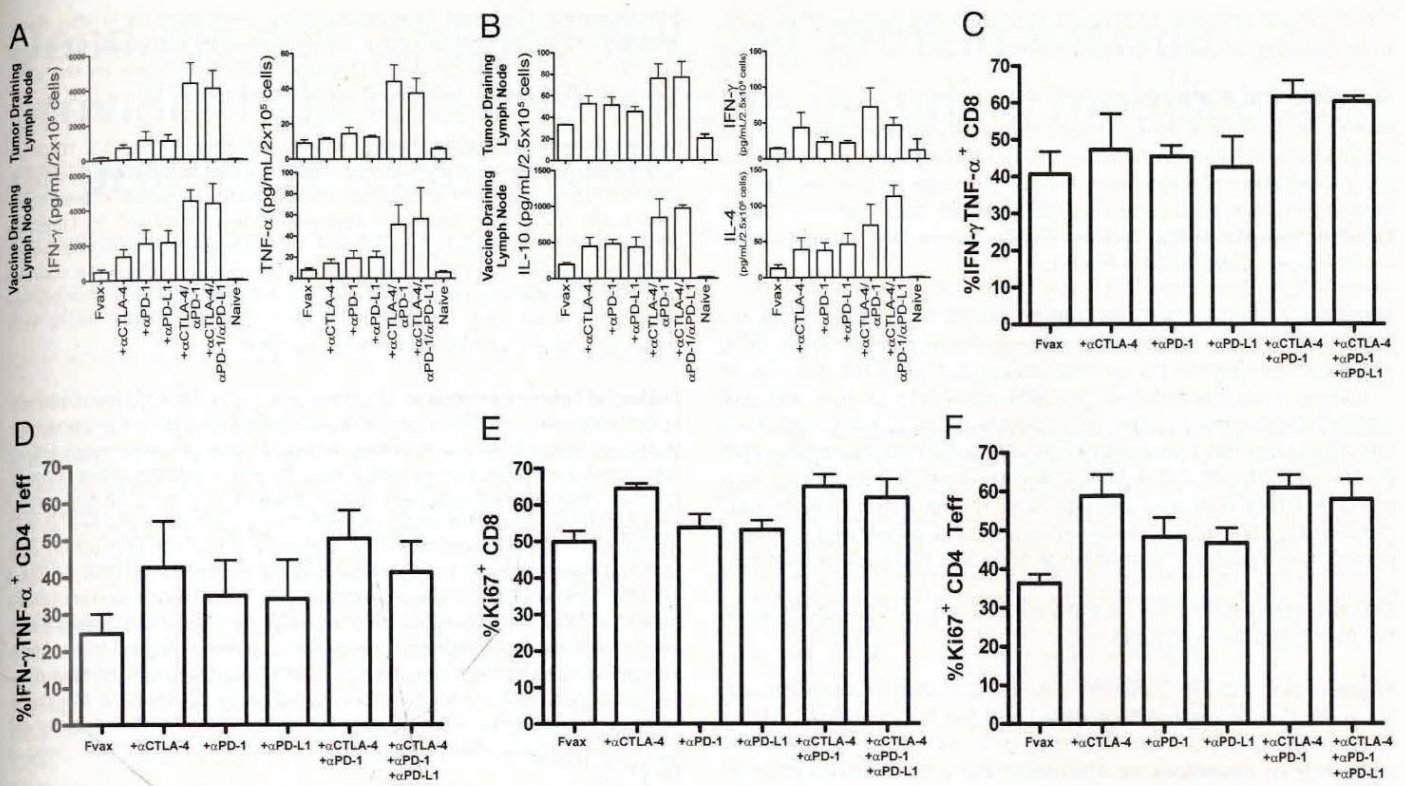


Fig. 5. Changes in cytokine production in response to coinhibitory blockade. Mice challenged with 2.5×10^5 B16-Ova cells and treated on days 6, 9, and 12 were killed on day 14. T cells were purified from tumor-draining lymph nodes and vaccine-draining lymph nodes, stained with antibodies, and sorted by flow cytometry into $CD4^+$ and $CD8^+$ subsets. Cytokine production was measured after 36 h using the TH1/TH2/TH17 CBA Kit and is shown for 2×10^5 CD8 T cells restimulated on 1×10^5 Ova 257–264 peptide-pulsed DCs (*A*) and for 2.5×10^5 CD4 T cells restimulated on 1×10^5 Ova 323–339 peptide-pulsed DCs (*B*). Data are shown for three to four independent experiments with five pooled mice per group. (*C* and *D*) TILs were purified from 5–10 pooled tumors per group and enriched using the Miltenyi T-cell purification kit. A total of 2×10^6 TILs were restimulated with 7.5×10^5 DCs [1:1 mix of Ova(257) and Ova(323) pulsed DCs] per well for 8 h in the presence of GolgiPlug. Cells were fixed using the FoxP3 kit and analyzed by flow cytometry for lymphocyte markers and intracellular IFN-γ and TNF-α production for CD8 cells (*C*) and CD4 Teffs (*D*) and also for Ki67 expression in CD8 cells (*E*) and CD4 Teffs (*F*). TIL data are from four independent experiments. All means shown are ± SEM.

with Gvax suggests the presence of a dominant suppressive mechanism. We have observed that Gvax, even when administered on the opposite flank from the tumor site, leads to increased myeloid suppressor accumulation in the tumor, although Fvax can have the opposite effect (6). Gvax may also increase elaboration of tolerogenic cytokines such as TGF-β (24). Additionally, Fvax has been shown to elicit greater CD8 infiltration of both vaccine and tumor sites relative to Gvax, which may also be partially responsible for the increased synergy with therapies such as αPD-1, which interact strongly with CD8 T cells. It is also possible that the optimal timing of coinhibitory blockade may differ in the context of Gvax vs. Fvax. In the end, further study will be necessary to define the reasons underlying the lack of cooperativity between CTLA-4/PD-1 combination blockade and Gvax.

Although we observe enhanced infiltration, activation marker expression, and inflammatory cytokine production following simultaneous blockade of the CTLA-4 and PD-1 pathways, the greatest difference between single and multiple coinhibitory blockade was in enhancing the ratio of $CD8^+$ T cells relative to Tregs and MDSCs in tumors. In each case, ratios following combination antibody treatment were more than double those from mice receiving any single antibody and ≈10-fold higher than those found in untreated mice. In the case of CD8/Treg ratios, the cooperativity we observe likely results from increased CD8 infiltration and expansion, impaired conversion of CD4 T cells into Tregs resulting from CTLA-4 blockade, and reduced Treg suppression through PD-1 blockade (15, 25). In the case of MDSCs, enhanced production of Th1-type cytokines by the increased fraction of tumor-infiltrating T cells likely antagonizes further MDSC formation, although converting a portion of the tumor-infiltrating myeloid cells into functional APCs at the same time. Supporting this model, we found that combination coinhibitory blockade significantly reduced the fraction of TILs composed of MDSCs (Fig. S10). Direct antagonism of MDSC function through coinhibitory blockade has been reported in ovarian cancer; however, we observed minimal expression of PD-1 and CTLA-4 by these cells in untreated B16 tumors (26) (Fig. S11). PD-L1, in contrast, was expressed by a substantial portion of MDSCs, making it impossible for us to exclude direct effects on these cells in mice receiving αPD-L1 antibody. Anti-PD-L1 alone, however, did not appear to have a substantially greater impact on MDSC-to-T-cell ratios than other coinhibitory blocking antibodies (Fig. 4). This striking reversal in the ratios of $CD8^+$ T cells to suppressor T and myeloid cells within the tumor is largely responsible for shifting the microenvironment from one of dominant suppression to an inflammatory milieu permissive for immune-mediated tumor rejection.

In clinical trials, antibodies that block CTLA-4 have shown efficacy in treating advanced melanoma and prostate cancer but at the price of autoimmune complications that are often severe. Human studies of αPD-1 and αPD-L1 antibodies are at a much earlier stage yet suggest that these agents may be efficacious while engendering fewer autoimmune complications (27). Our preclinical data in the B16 melanoma model strongly suggest that combining these agents may have synergistic effects in driving tumor rejection. Although combining multiple coinhibitory blocking antibodies in the clinic should be approached with great caution, our studies suggest that blocking a single inhibitory receptor only leads to up-regulation of the unblocked pathway. To allow tumor-infiltrating T cells the capacity to expand, kill, and produce inflammatory cytokines within the tumor micro-

environment appears to require simultaneous blockade of multiple negative costimulatory receptors.

Materials and Methods

Mice. C57BL/6 mice (4–6-week-old male; Jackson Laboratories) were cared for accordance with National Institutes of Health and American Association for the Accreditation of Laboratory Animal Care International regulations. Experiments were all approved by the Memorial Sloan-Kettering Cancer Center Institutional Animal Care and Use Committee. B6.SJL mice (6-week-old male) were obtained from Taconic.

Antibodies. Anti-CTLA-4 (9D9), αPD-1 (RMP1-14) (28), αPD-L1 (9G2), Rat Ig, and mIgG2b used in vivo were obtained from Bioxcell. Dosing per injection was 100 μg of 9D9, 250 μg of RMP114, 100 μg of 9G2, 250 μg of Rat Ig, and 100 μg of mIgG2b.

Staining antibodies included CD4-Q605, CD8-Pacific Orange, and CD3-APCAlexa750 (Invitrogen); CD4-APC, FoxP3-Pacific Blue, KLRG1-APC, PD-1-FITC, 4-1BB-biotin, GR-1-phycoerythrin (PE) Cy7, and CD11b (eBioscience); CD8-PE, PD-L1-PE, IFN-γ-PE-CY7, Ki67-FITC, and TNF-α-APC (BD Bioscience); ICOS and CTLA-4 (4F10) (Bioxcell); CD45.1 peridinin chlorophyll protein (Biolegend); and arginase-1 (Santa Cruz). Some clones were conjugated using Invitrogen monoclonal antibody conjugation kits to Alexa 532, Alexa 594, or Qdot 655.

Cell Lines. B16/BL6 cells as well as B16-sFlt3L-Ig (Fvax) and B16-GM-CSF (Gvax) have been described previously.

Peptides. Ova 257–264 (SIINFEKL) and 323–339 (ISQAVHAAHAFINEAGR) (American Peptide Company) were used at a final concentration of 5 μM. GP100 (25), Trp-1 (455, 481, and 522), and Trp-2 (181) peptides were obtained from Biosynthesis, Inc. and used at a final concentration of 10 μm.

B16 Melanoma Treatment Experiments. Mice were injected in the flank intradermally at day 0 with 5×10^4 B16-BL6 cells and treated on days 3, 6, and 9, with 1×10^6 irradiated (150 Gy) gene-modified B16 cells on the contralateral flank and the indicated therapeutical antibody i.p.

Tumor Infiltration/Activation Marker Analysis. Mice receiving a 1.5×10^5 B16-BL6 challenge were vaccinated as discussed in the previous section on days 3, 6, and 9 and were killed on day 16. Tumors were measured immediately before the mice were killed. Excised tumors were digested in Liberase (Roche) and DNase (Roche), cells were counted, and lymphocytes were enriched on a Ficoll gradient (Histopaque 1119; Sigma). Cells were stained using a FoxP3 staining kit (eBioscience); CTLA-4 and PD-1 were stained for total intracellular and extracellular protein. Stained samples were run completely on an LSRII (BD Bioscience) cytometer.

Analysis of Cytokine Production. Mice receiving a 2.5×10^5 B16-Ova challenge in 30% collagen matrix (Matrigel) were vaccinated as discussed in the previous section on days 6, 9, and 12 and killed on day 14. Vaccine and tumor draining lymph nodes as well as tumors were pooled from five mice per group. Lymph node cells were stained with DAPI and antibodies to CD4 and CD8 and sorted on a MoFlo cell sorter (Beckman Coulter). Tumor cells were purified as discussed previously except that before restimulation, the T-cell fraction was enriched using a Miltenyi T-cell purification kit. A total of 2×10^5 CD8 cells and 2.5×10^5 CD4 cells per well were restimulated in 96-well round-bottom plates with 1×10^5 Ova peptide-pulsed DCs purified from B6.SJL mouse spleens using $CD11c^+$ selection beads (Miltenyi) for 36 h, and cytokine production was then assessed using a TH1/TH2/TH17 CBA kit from BD Bioscience. For tumor samples, 2×10^6 T-enriched TILs were restimulated with 7.5×10^5 Ova and B16 melanoma peptide-pulsed DCs for 8 h in the presence of GolgiPlug (BD Bioscience) and then fixed and stained for intracellular cytokine production using a FoxP3 kit.

1. Linsley PS, et al. (1991) Binding of the B cell activation antigen B7 to CD28 costimulates T cell proliferation and interleukin 2 mRNA accumulation. *J Exp Med* 173:721–730.
2. Peggs KS, Quezada SA, Allison JP (2008) Cell intrinsic mechanisms of T-cell inhibition and application to cancer therapy. *Immunol Rev* 224:141–165.
3. Butte MJ, Keir ME, Phamduy TB, Sharpe AH, Freeman GJ (2007) Programmed death-1 ligand 1 interacts specifically with the B7-1 costimulatory molecule to inhibit T cell responses. *Immunity* 27:111–122.
4. Gabrilovich DI, Nagaraj S (2009) Myeloid-derived suppressor cells as regulators of the immune system. *Nat Rev Immunol* 9:162–174.
5. Okazaki T, Honjo T (2007) PD-1 and PD-1 ligands: From discovery to clinical application. *Int Immunol* 19:813–824.
6. Curran MA, Allison JP (2009) Tumor vaccines expressing Flt3 ligand synergize with CTLA-4 blockade to reject preimplanted tumors. *Cancer Res* 69:7747–7755.
7. van Elsas A, Hurwitz AA, Allison JP (1999) Combination immunotherapy of B16 melanoma using anti-cytotoxic T lymphocyte-associated antigen 4 (CTLA-4) and granulocyte/macrophage colony-stimulating factor (GM-CSF)-producing vaccines induces rejection of subcutaneous and metastatic tumors accompanied by autoimmune depigmentation. *J Exp Med* 190:355–366.
8. Nishimura H, Nose M, Hiai H, Minato N, Honjo T (1999) Development of lupus-like autoimmune diseases by disruption of the PD-1 gene encoding an ITIM motif-carrying immunoreceptor. *Immunity* 11:141–151.
9. Tivol EA, et al. (1995) Loss of CTLA-4 leads to massive lymphoproliferation and fatal multiorgan tissue destruction, revealing a critical negative regulatory role of CTLA-4. *Immunity* 3:541–547.
10. Parry RV, et al. (2005) CTLA-4 and PD-1 receptors inhibit T-cell activation by distinct mechanisms. *Mol Cell Biol* 25:9543–9553.
11. Fife BT, et al. (2009) Interactions between PD-1 and PD-L1 promote tolerance by blocking the TCR-induced stop signal. *Nat Immunol* 10:1185–1192.
12. Rudd CE (2008) The reverse stop-signal model for CTLA4 function. *Nat Rev Immunol* 8: 153–160.
13. Mach N, et al. (2000) Differences in dendritic cells stimulated in vivo by tumors engineered to secrete granulocyte-macrophage colony-stimulating factor or Flt3-ligand. *Cancer Res* 60:3239–3246.
14. Quezada SA, Peggs KS, Curran MA, Allison JP (2006) CTLA4 blockade and GM-CSF combination immunotherapy alters the intratumor balance of effector and regulatory T cells. *J Clin Invest* 116:1935–1945.
15. Wang W, et al. (2009) PD1 blockade reverses the suppression of melanoma antigen-specific CTL by CD4+ CD25(Hi) regulatory T cells. *Int Immunol* 21:1065–1077.
16. Zheng SG, et al. (2006) TGF-beta requires CTLA-4 early after T cell activation to induce FoxP3 and generate adaptive CD4+CD25+ regulatory cells. *J Immunol* 176:3321–3329.
17. Beyersdorf N, Ding X, Tietze JK, Hanke T (2007) Characterization of mouse CD4 T cell subsets defined by expression of KLRG1. *Eur J Immunol* 37:3445–3454.
18. Zhang P, et al. (2007) Agonistic anti-4-1BB antibody promotes the expansion of natural regulatory T cells while maintaining Foxp3 expression. *Scand J Immunol* 66: 435–440.
19. Herman AE, Freeman GJ, Mathis D, Benoist C (2004) CD4+CD25+ T regulatory cells dependent on ICOS promote regulation of effector cells in the prediabetic lesion. *J Exp Med* 199:1479–1489.
20. Linton PJ, et al. (2003) Costimulation via OX40L expressed by B cells is sufficient to determine the extent of primary CD4 cell expansion and Th2 cytokine secretion in vivo. *J Exp Med* 197:875–883.
21. Nakamoto N, et al. (2009) Synergistic reversal of intrahepatic HCV-specific CD8 T cell exhaustion by combined PD-1/CTLA-4 blockade. *PLoS Pathog* 5:e1000313.
22. Iwai Y, et al. (2002) Involvement of PD-L1 on tumor cells in the escape from host immune system and tumor immunotherapy by PD-L1 blockade. *Proc Natl Acad Sci USA* 99:12293–12297.
23. Li B, et al. (2009) Anti-programmed death-1 synergizes with granulocyte macrophage colony-stimulating factor–secreting tumor cell immunotherapy providing therapeutic benefit to mice with established tumors. *Clin Cancer Res* 15:1623–1634.
24. Jinushi M, et al. (2007) MFG-E8-mediated uptake of apoptotic cells by APCs links the pro- and antiinflammatory activities of GM-CSF. *J Clin Invest* 117:1902–1913.
25. Peggs KS, Quezada SA, Chambers CA, Korman AJ, Allison JP (2009) Blockade of CTLA-4 on both effector and regulatory T cell compartments contributes to the antitumor activity of anti-CTLA-4 antibodies. *J Exp Med* 206:1717–1725.
26. Liu Y, et al. (2009) Regulation of arginase I activity and expression by both PD-1 and CTLA-4 on the myeloid-derived suppressor cells. *Cancer Immunol Immunother* 58: 687–697.
27. Berger R, et al. (2008) Phase I safety and pharmacokinetic study of CT-011, a humanized antibody interacting with PD-1, in patients with advanced hematologic malignancies. *Clin Cancer Res* 14:3044–3051.
28. Yamazaki T, et al. (2005) Blockade of B7-H1 on macrophages suppresses CD4+ T cell proliferation by augmenting IFN-gamma-induced nitric oxide production. *J Immunol* 175:1586–1592.